Flux variations and vertical distributions of siliceous Rhizaria (Radiolaria and Phaeodaria) in the western Arctic Ocean: indices of environmental changes

Takahito Ikenoue [a, b, c, *], Kjell R. Bjørklund [b], Svetlana B. Kruglikova [d], Jonaotaro Onodera [c], Katsunori Kimoto [c], Naomi Harada [c]

a: Department of Earth and Planetary Sciences, Graduate School of Sciences, Kyushu University, 6-10-1 Hakozaki, Higashi-ku, Fukuoka 812-8581, Japan

b: Natural History Museum, Department of Geology, University of Oslo, P.O. Box 1172 Blindern, 0318 Oslo, Norway

c: Research and Development Center for Global Change, JAMSTEC, Natsushima-cho 2-15, Yokosuka, 237-0061, Japan.

d: P.P. Shirshov Institute of Oceanology, Russian Academy of Sciences, Nakhimovsky Prospect 36, 117883 Moscow, Russia

*Corresponding author; Present address: Central Laboratory, Marine Ecology Research Institute, 300 Iwawada, Onjuku-machi, Isumi-gun, Chiba 299-5105 Japan; E-mail: ikenoue@kaiseiken.or.jp

Abstract

The vertical distribution of radiolarians was investigated using a vertical multiple plankton sampler (100−0, 250−100, 500−250 and 1,000−500 m water depths, 62 μm mesh size) at the Northwind Abyssal Plain and southwestern Canada Basin in September 2013. To investigate seasonal variations in the flux of radiolarians in relation to sea ice and water masses, a time series sediment trap system was moored at Station NAP (75°00'N, 162°00'W, bottom depth 1,975 m) in the western Arctic Ocean during October 2010–September 2012. The radiolarian flux was comparable to that in the North Pacific Ocean. *Amphimelissa setosa* was dominant during the season with open water as well as at the beginning and at the end of the seasons with sea-ice cover. During the sea-ice cover season, however, oligotrophic and cold-water tolerant

actinommids were dominant, productivity of radiolaria was lower, and species diversity was greater. These suggest that the dynamics of sea ice are a major factor affecting the productivity, distribution, and composition of the radiolarian fauna.

Keywords: Radiolarians, Western Arctic Ocean, Sea-ice, Beaufort Gyre, Sediment trap

1. Introduction

In recent years, summer sea-ice extent in the Arctic Ocean has decreased rapidly due to global climate change (Stroeve et al., 2007, 2012). The sea ice in the Arctic Ocean reached its minimum extent in September 2012; the lowest since the beginning of satellite observations (NSIDC, 2012). The most remarkable sea-ice decrease was observed in the western Arctic Ocean, on the Pacific side (Shimada et al., 2006; Comiso et al., 2008; Markus et al., 2009). In the western Arctic Ocean, the advection of warm North Pacific water through the Bering Strait contributes to both sea-ice melt in summer and an inhibition of sea-ice formation during winter (Shimada et al., 2006; Itoh et al., 2013).

Biological CO_2 absorption is an important carbon sink in the ice-free regions of the Arctic Ocean (Bates et al., 2006; Bates and Mathis, 2009). Melting of sea-ice can both enhance and reduce the efficiency of the biological pump in the Arctic Ocean, depending on ocean circulation (Nishino et al., 2011). The Beaufort High, a high-pressure system over the Canada Basin in the Arctic Ocean, drives the sea ice and the water masses anticyclonically, forming the Beaufort Gyre (Fig. 1). In the Canada Basin, the Beaufort Gyre governs the upper ocean circulation (Proshutinsky et al., 2002), and it has strengthened recently due to the decreasing sea ice (Shimada et al., 2006; Yang, 2009). Melting of sea ice reduces the efficiency of the biological pump within the Beaufort Gyre, due to deepening of the nutricline caused by freshwater accumulation within the gyre (Nishino et al., 2011). Conversely, the efficiency of the biological pump is enhanced outside the gyre because of nutrient supply from shelves and improved light penetration (Nishino et al., 2011).

Particle flux plays an important role in the carbon export (Francois et al., 2002). Based on sediment trap samples from the Canada Basin and Chukchi Rise, Honjo et al. (2010) found that the annual average of sinking particle flux was three orders of magnitude smaller than that in epipelagic areas where the particle flux was the main

mechanism for carbon export to greater depths. However, Arrigo et al. (2012) observed a massive algal biomass beneath fully consolidated pack ice far from the ice edge in the Chukchi Sea during the summer, and suggested that a thinning ice cover increased light transmission under the ice and allowed blooming of algae. Boetius et al. (2013) also reported that the algal biomass released from the melting ice in the Arctic Ocean was widely deposited at the sea floor in the summer of 2012. Therefore, it is inferred that the biomass of zooplankton, that were preying on the algae, also changed seasonally under the sea ice in the Arctic Ocean, as a result of the variable sea-ice conditions. Microzooplankton are recognized as a key component of pelagic food webs (e.g., Kosobokova et al., 2002; Calbet and Landry, 2004), but the seasonal and interannual changes in their communities within sea-ice regions are still poorly understood.

To understand the effect of sea-ice reduction on marine ecosystems in the Arctic Ocean, we studied productivity, distribution, composition, and biological conditions of living radiolarians in both plankton tow samples and sediment trap samples.

In our study, we have analyzed only the siliceous taxa of the class Rhizaria; and herein we have used the definition of Radiolaria to include them as defined by Suzuki and Aita (2011). In their taxonomic scheme, they include the following orders: Collodaria, Nassellaria, Spumellaria, Acantharia and Taxopodia. In addition, we also include the order Entactinaria, which Suzuki and Aita (2011) reported became extinct during the Permian; but Bjørklund et al. (2008) demonstrated its presence also in recent plankton and sediment samples. In this study, we have excluded the order Acantharia as they have a skeleton of $SrSO_4$; and also Collodaria, a group that normally does not possess a skeleton, or only with loose spines. Therefore, our study only includes forms with a solid skeleton of SiO_2. In this paper, we have chosen to include data also for the order Phaeodaria, which are no longer assigned to Radiolaria, but to Cercozoa based on recent molecular phylogenetic studies (Cavalier-Smith and Chao, 2003; Nikolaev et al., 2004; Adl et al., 2005; Yuasa et al., 2005). To make the text read more easily, we therefore use Radiolaria, or radiolarians when appropriate, to also include Phaeodaria. This is also intended to make it possible for us to compare previously published data from the north Pacific region, where the Phaeodaria were included among the Radiolaria (Okazaki et al., 2003, 2005; Ikenoue et al., 2010, 2012a).

Radiolaria are one of the most common marine microzooplankton groups, they secrete siliceous skeletons, and their species-specific abundance in a region is related to

temperature, salinity, productivity and nutrient availability (Anderson, 1983; Bjørklund et al., 1998; Cortese and Bjørklund, 1997; Cortese et al., 2003). Their genus and family levels taxa also respond to various oceanographic conditions by altering their distribution patterns and compositions (Kruglikova et al., 2010, 2011). In recent studies, Ikenoue et al. (2012a, b) found a close relationship between water mass exchanges and radiolarian abundances based on a fifteen-year-long, time-series observation on radiolarian fluxes in the central subarctic Pacific. Radiolarian assemblages are also related to the vertical hydrographic structure (e.g., Kling, 1979; Ishitani and Takahashi, 2007; Boltovskoy et al., 2010); therefore, variations in their abundance and proportion might be useful environmental proxies for water mass exchanges at each depth interval, especially because some of them occur in response to recent climate change (e.g., ocean circulation, expansion and decline of sea ice, and influx of water mass from other regions).

The radiolarian assemblages in the western Arctic Ocean have been studied mainly based on the samples collected by plankton tows at ice-floe stations (Hülsemann, 1963; and Tibbs, 1967), and in the Beaufort Sea in summer of 2000 (Itaki et al., 2003); or in surface sediment samples, mainly over the Atlantic side of the Arctic Ocean (Bjørklund and Kruglikova, 2003). Bernstein (1931, 1932, 1934) reported on the presence of six Polycystina, two Acantharia and two Taxopodia species, but did not give any information on abundance in the Barents Sea and Kara Sea for the Polycystina. However, she reported that Acantharia and Taxopodia were abundant, with a maximum occurrence in the deeper and warmer Atlantic water. Meunier (1910) also reported on Acantharia, Taxopodia and Nassellaria in the Kara Sea and the Arctic Ocean, but he stated (page 196) that his material was not rich in radiolarians. However, the knowledge of the geographical and the depth distribution of living radiolarians is still limited, and their seasonal and annual changes have not been studied in the western Arctic Ocean in relation to seasonal sea-ice coverage.

This is the first extensive study of the seasonal and interannual flux changes of radiolarians in the western Arctic Ocean. We present radiolarian depth distributions and flux variations in the western Arctic Ocean, and discuss their seasonality and species associations in relation to the environmental conditions (temperature, salinity, depth, sea-ice concentration, and downward shortwave radiation).

2. Oceanographic setting

The hydrography in the western Arctic Ocean has been discussed in several studies (e.g., Aagaard et al., 1985; McLaughlin et al., 2011) and the upper 1,000 m of the water column can be divided into five distinct water masses. The surface water is characterized by low temperature and low salinity water (Aagaard et al., 1981) and can be subdivided into three layers, i.e. Surface Mixed Layer (SML), Pacific Summer Water (PSW), Pacific Winter Water (PWW). The SML (0-25 m) is formed in summer by sea-ice melt and river runoff, and is characterized by low salinities (less than 28). The PSW (25-100 m) and PWW (100-250 m) are cold, halocline layers originating from the Pacific Ocean via the Bering Sea. The PSW flows along the Alaskan coast and enters the Canada Basin through the Bering Strait and Barrow Canyon (Coachman and Barnes, 1961) (Fig. 1). The PSW is relatively warmer and less saline (30-32 in the 1990s, 28-32 in the 2000s) than the PWW (Jackson et al., 2011). The PSW is further classified into warmer and less saline Alaskan coastal water and cooler and more saline Bering Sea water (Coachman et al., 1975), which originate from Pacific water that is modified in the Chukchi and Bering Seas during summer. The Alaskan coastal water is carried by a current along the Alaskan coast, and spreads northwards along the Northwind Ridge by the Beaufort gyre depending on the rates of ice cover and decay (Shimada et al., 2001). The PWW is characterized by a temperature minimum (of about −1.7°C) and originates from Pacific water that is modified in the Chukchi and Bering Seas during winter (Coachman and Barnes, 1961). The PWW is also characterized by a nutrient maximum, and its source is regenerated nutrients from the shelf sediments (Jones and Anderson, 1986).

The deep water is divided into Atlantic Water (AW) and Canada Basin Deep Water (CBDW). The AW (250-900 m) is warmer (near or below 1°C), and saltier (near 35) than the surface waters, and originates from the North Atlantic Ocean, via the Norwegian Sea. The CBDW (below 900 m) is a cold (lower than 0°C) water mass located beneath the AW, and has the same salinity as the AW. The CBDW is formed by brine formation on the shelves, which makes the cold and dense saline water mass sink over the continental margin into the deep basins (Aagaard et al., 1985).

3. Materials and methods

3.1. Plankton tow samples

Plankton tow samples were collected using a vertical multiple plankton sampler (VMPS). The instrument (mesh size: 62 μm, open mouth area: 0.25 m^2) was towed from four layers (100-0, 250-100, 500-250, and 1,000-500 m) at two stations (Station 32 in the Northwind Abyssal Plain, 74°32'N, 161°54'W; Station 56 in southwestern Canada Basin, 73°48'N, 159°59'W) (Fig. 1 and Table 1) in September 2013. Hydrographical data (temperature, salinity, dissolved oxygen, and chlorophyll *a*) down to 1,000 m water depth were simultaneously obtained from a CTD (Conductivity Temperature Depth profiler) cast. The volume of seawater filtered through the net was estimated using a flow meter mounted in the mouth ring of the plankton net.

The samples collected by VMPS were split with a Motoda box splitter and a rotary splitter (McLane^{TM}WSD-10). The split samples were fixed with 99.5% ethanol for radiolarian studies. Plankton samples were stained with Rose-Bengal to discriminate between living and dead specimens. The split samples were sieved through a stainless steel screen with 45 μm mesh size. Remains on the screen were filtered through Gelman® membrane filters with a nominal pore size of 0.45 μm. The filtered samples were desalted with distilled water. The edges of each filtered sample were trimmed to fit a slide size while in a wet condition and mounted on glass slides on a slide warmer to dry. Xylene was added to the dried filters and samples, which were then permanently mounted with Canada balsam. Radiolarian taxa were identified and counted with a compound light microscope at 200x or 400x magnification. Specimens that clearly stained bright red were interpreted as living cells; while cells that did not stain red, or were just barely stained red, were interpreted as dead because they lacked sufficient intact protoplasm to absorb the stain. This is also in accordance to Okazaki et al. (2004). All specimens on a slide were identified and counted, and their individual numbers were converted to standing stocks (No. specimens m^{-3}).

3.2. Hydrographic profiles

Profiles of temperature, salinity, dissolved oxygen, and chlorophyll *a* down to 1,000 m depth at stations 32 (Northwind Abyssal Plain) and 56 (southwestern Canada Basin) in September 2013 (Nishino, 2013) were shown in Fig. 2a and b, respectively. At Station 32, temperature showed a sharp decrease from the surface, down to about 25 m depth with a sharp increase at the base of the SML. The PSW is generally cold (about −1°C) with a maximum value (1.6°C) at about 50 m and shows a rapid decrease with

increasing depth. The PWW is the coldest water (minimum value −1.6°C) at about 200 m. The highest temperatures are found in the AW (near or below 1°C) at about 400 m with a gradual decrease below 500 m. Salinity values (25-28) are low in the SML, increasing rapidly with depth from 28-32 in the PSW. In the PWW there is a gradual increase of salinity from 32 to 35, while there is a slight decrease below the PWW/AW boundary. Dissolved oxygen was maximum (405 µmol/kg) at the boundary between SML and PWW, rapidly decreased with increasing depth in the PSW and PWW, and reached a minimum value (270 µmol/kg) around the boundary between PWW and AW, and increased slightly below that. Chlorophyll *a* concentrations, higher than 0.1 mg m^{-3}, were observed in the 0-80 m depth. Temperature, salinity, dissolved oxygen, and chlorophyll *a* were almost similar at both Station 32 and Station 56, except for SML and PSW. In the SML, salinity at Station 32 was slightly lower than at Station 56. In the PSW, a temperature peak at Station 32 was about one degree higher, and a little deeper, compared to Station 56. In the 0-80 m depth, chlorophyll *a* was a little higher at Station 56 than at Station 32.

3.3. Sediment trap samples

Sinking particles were collected by a sediment trap (SMD26 S-6000, open mouth area 0.5 m^2, Nichiyu Giken Kogyo, Co. Ltd.) rotated at 10–15-day intervals moored at 184 m (4th October 2010–28th September 2011), 260 m (4th October 2011–18th September 2012), and 1,300 m (4th October 2010–28th September 2011), and 1,360 m (4th October 2011–18th September 2012) at Station NAP (Northwind Abyssal Plain, 75°00'N, 162°00'W, bottom depth 1,975 m) (Fig. 1; Table 2). The mooring system was designed to set the collecting instrument at approximately 600 m above the sea floor. This depth of the moored sediment traps was chosen in order to avoid possible inclusion of particles from the nepheloid layer, reaching about 400 m above the seafloor (Ewing and Connary, 1970). Recoveries and redeployments of the traps were carried out on the Canadian Coast Guard Ship I/B (ice breaker) “Sir Wilfrid Laurier” and R/V “Mirai” of the Japan Agency for Marine-Earth Science and Technology. The sample cups were filled with 5% buffered formalin seawater before the sediment trap was deployed. This seawater was collected from 1,000 m water depth in the southern Canada Basin, and was membrane filtered (0.45 µm pore size). The seawater in the sample cups was mixed with sodium borate as a buffer (pH 7.6–7.8) with 5% formalin added as a preservative.

The samples were first sieved through 1 mm mesh to remove larger particles, which are not relevant for the present study. The samples were split with a rotary splitter (McLane^{TM}WSD-10). At first, we used 1/100 aliquot size of the samples to make microslides for microscope work (species identification). We made additional slides in case there were low radiolarian specimen numbers. In order to remove organic matter and protoplasm, 20 ml of 10% hydrogen peroxide solution were added to the samples in a 100 ml Pyrex beaker, and heated (not boiling) on a hot plate for one hour. After this reaction was completed, Calgon® (hexametaphosphate, surfactant) solution was added to disaggregate the sample. The treated samples were then sieved through a screen (45 μm mesh size). Both the coarse (>45 μm) and fine (<45 μm) fractions were filtered through Gelman membrane filters with a nominal pore size of 0.45 μm and desalted with distilled water. The edges of each filtered sample were trimmed to fit to slide size in wet condition and mounted on glass slides on a slide warmer to dry. Xylene was added to the dried filters and samples, which were then permanently mounted with Canada balsam.

We made slides of both the coarse (>45 μm) and the fine (<45 μm) fraction of each sample. For the enumeration of radiolarian taxa in this study, we counted all specimens of radiolarian skeletons larger than 45 μm encountered on a slide. Each sample was examined under an Olympus compound light microscope at 200x or 400x magnification for species identification and counting. The radiolarian flux (No. specimens $m^{-2}\,day^{-1}$) was calculated from our count data using the following formula:

$$\text{Flux} = N^{*}V/S/D \qquad (1)$$

where N is the counted number of radiolarians, V the aliquot size, S the aperture area of the sediment trap (0.5 m^2), and D the sampling interval (day). Diversity indices using the Shannon-Weaver log-base 2 formula (Shannon and Weaver, 1949) were calculated for total radiolarians

$$H = -\Sigma\, P_i \log_2 P_i \qquad (2)$$

where H is the diversity index, P is the contribution of species (relative abundance in total radiolaria) and i is the order of species.

As supplemental environmental data, the moored sediment trap depth and the water temperature (accuracy of ± 0.28°C) were monitored every hour (sensor type: ST-26S-T). Moored trap depth for the upper trap was inadvertently lowered by about 80 m during the second year (approximately 260 m depth) than during the first year (approximately

180 m depth), caused by entanglement of the mooring ropes. During July-August in 2012, the moored trap depth was lowered to about 300 m, because of intensified water currents (Fig. S1). Time-series data of sea-ice concentration around Station NAP during the mooring period were calculated from the sea-ice concentration data set (http://iridl.ldeo. columbia.edu/SOURCES/.IGOSS/.nmc/.Reyn_Smith OIv2/, cf. Reynolds et al., 2002).

3.4. Taxonomic note

The species described by Hülsemann (1963) under the name of *Tholospyris gephyristes* is not a member of the Spyridae. This species has been accepted as a Spyridae by most workers, but this species lacks the sagittal ring that is typical for the Spyridae. We have, therefore, assigned this species to the family Plagiacanthidae. We suggest this species be renamed to *Tripodiscium gephyristes* until a proper taxonomic analysis has been undertaken, and have used this designation hereafter.

4. Results

4.1. Radiolarians collected by plankton tows

A total of 43 radiolarian taxa (12 Spumellaria, three Entactinaria, 26 Nassellaria, and two Phaeodaria) were identified in the plankton tow samples (Table 3). We have observed taxopodians, but they have not been identified according to the two species as defined by Meunier (1910), nor have they been quantified. Furthermore, we have not been able to observe any collodarian individuals, although we cannot exclude their presence in the Arctic Ocean (Lovejoy et al., 2006; Lovejoy and Potvin, 2011). The numbers of individuals for each radiolarian taxon are in Tables S1 (Station 32) and S2 (Station 56).

4.1.1. Standing stocks and diversities of radiolarians

The abundance of living radiolarians at Station 32 was about two times higher than at Station 56 at each depth interval in the upper 500 m, the depth level at which the abundance of living radiolarians decreased with increasing water depth at both stations (Fig. 2a and b). The abundance of dead radiolarians also decreased with water depth at both stations, except for 100–250 m depth at Station 32 (Fig. 2a and b). The abundance

of dead radiolarians was generally higher than living radiolarians at both stations, except for in the 0–100 m depth at Station 32. The living radiolarian diversity index was low in the 0-100 m depth interval, increased with depth, reached a maximum at about 400 m, and then slightly decreased below 500 m depth at both stations.

At Station 32, *Amphimelissa setosa* (58%) and *Amphimelissa setosa* juvenile (22%) were dominant, while *Joergensenium* sp. A (6%), *Pseudodictyophimus clevei* (4%), Actinommidae spp. juvenile forms (3%), and *Actinomma leptodermum leptodermum* (1%) were common (Fig 3a). At Station 56 the Actinommidae spp. juvenile forms (38%) and *Amphimelissa setosa* (29%) were dominant, and *Actinomma leptodermum leptodermum* (6%), *Amphimelissa setosa* juvenile (6%), *Pseudodictyophimus clevei* (5%), and *Joergensenium* sp. A (4%) were common (Fig 3b). We defined the two-shelled forms of Actinommidae as juvenile. To be consistent, the three- and four-shelled forms were identified as adult. For the *Amphimelissa setosa* we defined those with only a cephalis as juveniles. Those with a well developed cephalis, and with a barely or well developed thorax, were defined as adult. Actinommidae spp. juvenile forms are mostly two-shelled juvenile forms of *Actinomma leptodermum leptodermum* and *Actinomma boreale*, making it impossible to separate between the two.

4.1.2. Vertical distribution of radiolarian species

We selected fourteen abundant radiolarian taxa to show their relation to the vertical hydrographic structure in the western Arctic Ocean (Fig. 4). The selected taxa were radiolarian taxa with 1% or higher relative abundance through the upper 1,000 m of the water column at either of the two stations and with high relative abundance in each water depth.

Adult and juvenile forms of *Amphimelissa setosa* were mainly distributed in the 0–250 m depth at both stations. In the 0-100 m depth, adult and juvenile stages were dominant (70% and 28%, respectively) at Station 32, and were abundant at Station 56 (23% and 7%, respectively), following the juvenile *Actinomma* spp. (56%). In the 100–250 m depth, *A. setosa* was the dominant species at both stations. At Station 32, the abundance of *A. setosa* in the 100–250 m depth interval was lower than in the 0–100 m depth, whereas at Station 56, the abundance in the 100-250 m depth was almost the same as in the 0–100 m depth.

Actinommidae spp. juvenile forms and *Actinomma l. leptodermum* were absent in

the 0–100 m depth at Station 32; but both, especially Actinommidae spp. juvenile forms (56%), were abundant at Station 56. Both were common in the 100-250 m depth at both stations (8% and 4%, respectively at Station 32; 14% and 7%, respectively at Station 56), and decreased in abundance in the 250–500 m depth. *Spongotrochus glacialis* was rare in the 0-100 m depth at Station 32 (0.4%) but with a slight increase at Station 56 (1.4%). In deeper layers *S. glacialis* was rare.

Joergensenium sp. A, *Pseudodictyophimus clevei,* and *Actinomma boreale* were abundant in the 100–250 m depth at both stations. *Joergensenium* sp. A was absent in the 0–100 m depth, but abundant in the 100–250 m depth, and rare in deeper depths. *Pseudodictyophimus clevei* was found throughout the water column from the surface to 1,000 m depth; but was rare at Station 32, except in the 100-250 m depth. *Actinomma boreale* was rare and mainly found in the 100–250 m depth at both stations.

Ceratocyrtis histricosus was mainly found in the 250–500 m depth, and occurred also in the 100–250 m depth at both stations. *Tripodiscium gephyristes* was widely distributed below 100 m depth at Station 56; while at Station 32, this species was scarce at all depth layers. *Pseudodictyophimus g. gracilipes* occurred in very low numbers at both stations through the upper 1,000 m. *Pseudodictyophimus plathycephalus*, Plagiacanthidae gen. et sp. indet., and *Cycladophora davisiana* were most abundant below 500 m depth at both stations.

4.2. Radiolaria collected by sediment trap

A total of 51 radiolarian taxa (15 Spumellaria, three Entactinaria, 31 Nassellaria, and two Phaeodaria) were identified in the upper and lower sediment trap samples at Station NAP during 4th October 2010–18th September 2012 (Table 3). We have observed taxopodians, but they have not been identified nor quantified. Furthermore, we have not been able to observe any collodarian individuals. The number of radiolarians counted in each sample ranged from eight to 1,100 specimens in the upper trap, and from 0 to 2,672 specimens in the lower trap (Tables S3 and S4). There were 15 samples with fewer than 100 specimens (two samples in the upper trap, and 13 samples in the lower trap). Most of the species recognized in our sample materials are shown in Plates 1-9.

4.2.1. Radiolarian flux and diversity in the upper trap

The highest total radiolarian fluxes in the upper trap were observed during the beginning of the sea-ice cover season (November in 2010 and 2011, >10,000 specimens m^{-2} day^{-1}) (Fig. 5). The fluxes were higher during the open-water season (August–October in 2011; average, 5,710 specimens m^{-2} day^{-1}), and around the end of the sea-ice cover season (July–August in 2011, >4,000 specimens m^{-2} day^{-1}) than during the sea-ice cover season (December–June, average in 2011, 944 specimens m^{-2} day^{-1}; average in 2012, 723 specimens m^{-2} day^{-1}). The fluxes varied from 114 to 14,677 specimens m^{-2} day^{-1} with an annual mean of 2,823 specimens m^{-2} day^{-1}. The diversity of radiolarians, however, was higher during the sea-ice cover season (>3) than during the open water season (<2) (Fig. 5). The diversity indices were negatively correlated with the total radiolarian fluxes ($r = -0.91$) (Fig. 6).

Species composition varied seasonally. Adult and juvenile *Amphimelissa setosa* were most dominant (90%) during the sea-ice free season, and the beginning and the end of sea-ice cover season. The juvenile and adult forms were abundant in earlier and later seasons, respectively (Fig. 7). During the sea-ice cover season, however, Actinommidae spp. juvenile forms (range, 0–51%; average, 18%), *Actinomma leptodermum leptodermum* (range, 0–14.6%; average, 4%), *Actinomma boreale* (range, 0–33%; average, 4%) were dominant. Relatively high percentages of *Pseudodictyophimus clevei*, *Pseudodictyophimus gracilipes*, and *Tripodiscium gephyristes* were also observed during the sea-ice cover season.

4.2.2. Radiolarian flux and diversity in the lower trap

Total radiolarian flux in the lower trap varied from 0 to 22,733 specimens m^{-2} day^{-1} with an annual mean of 4,828 specimens m^{-2} day^{-1} (Fig. 5). The fluxes were high during November–December, both in 2010 and 2011 and during March in 2011 (>10,000 specimens m^{-2} day^{-1}), while extremely low (average, 21 specimens m^{-2} day^{-1}) during May-September in 2012. Diversity did not change greatly, and increased slightly, during May-July 2011, and in April 2012 when the radiolarian fluxes were low. The diversity indices were weakly negatively correlated with the radiolarian fluxes ($r = -0.52$) (Fig. 6).

Adult and juvenile stages of *Amphimelissa setosa* were dominant throughout the sampling periods (range, 66–92%; average, 82%). The relative abundance of *A. setosa* juveniles was slightly increased in 2012 in comparison to 2010 and 2011.

5. Discussion

5.1. Comparison between Arctic and North Pacific Oceans

Biogenic particle flux into the deep sea in the Canada Basin was generally assumed to be low due to the low productivity of siliceous and calcareous microplankton (Honjo et al., 2010). However, we observed high radiolarian fluxes (14,677: upper trap, 22,733: lower trap) at Station NAP during the open-water season, and around the beginning and the end of the sea-ice cover season in 2011-2012. The annual means (2,823: upper trap, 4,823: lower trap) were comparable to those observed in several areas of the North Pacific Ocean (Fig. 8, Table S5). The radiolarian flux in the upper trap was high during July-November and low during December-June. Moreover, radiolarian flux in the lower trap was extremely low during May-September 2012. The mean of radiolarian fluxes during the period when radiolarian fluxes were higher than 1σ (3,489: upper trap; 5,675: lower trap) showed a higher value (7,344: upper trap; 11,871: lower trap) than at any other stations in the North Pacific Ocean (Table S5). The biogenic opal collected in this study mainly consisted of radiolarians and diatoms based on our microscopic observations. Other siliceous skeletons (silicoflagellate skeletons, siliceous endoskeleton of dinoflagellate genus *Actiniscus*, chrysophyte cysts, ebridian flagellates, and palmales) were minor components in the same trap samples (Onodera et al., 2014). Although more than half of the contribution to total particulate organic carbon is largely unknown at station NAP (Onodera et al. 2014), our study showed that the siliceous skeletons of radiolarians and diatoms might play an important role in the export of biogenic silica to the deep Arctic Ocean.

5.2. Vertical distribution of species and hydrographic structure

5.2.1. PSW and PWW association

Amphimelissa setosa and its juvenile stages were found in shallow cold-water in both stations 32 and 56. Specifically, they were more abundant in the SML and PSW (0-100 m) at Station 32 than Station 56. At Station 32, these two water masses exhibited warmer temperature (about one degree higher at the temperature peak) than Station 56; indicating that cold to moderately warm (-1.2 to 1.6ºC), and well mixed water masses were more favorable for this species than perennial cold water masses such as PWW (100-250 m). Dolan et al. (2014) showed that density of *A. setosa* in the Chukchi Sea

was lower in 2012, when sea ice coverage was less and chlorophyll *a* concentrations were higher, than in 2011. Thus, the density of phytoplankton protoplasm containing chlorophyll *a* might not be related to the abundance of *A. setosa*. This is consistent with our finding that the abundance of *A. setosa* was fairly lower at Station 56 where density of chlorophyll *a* was a little higher than that at Station 32. Thus, the favorable condition for *A. setosa* is related to a cold and well mixed water mass in the summer sea-ice edge.

A. setosa dominated (60-86%) the radiolarian assemblage through the upper 500 m of the water column in the Chukchi Sea and the Beaufort Sea, and thus can be an indicator of cold Arctic surface water (Itaki et al., 2003). Bernstein (1931) noted that this species lives in the cold (-1.68 to -1.29ºC) and saline (34.11 to 34.78) waters in the Arctic Ocean. Matul and Abelmann (2005) also suggested that *A. setosa* prefers well-mixed, cold and saline surface/subsurface waters.

Actinommidae spp. juvenile forms, *Actinomma l. leptodermum* and *Spongotrochus glacialis* were mainly distributed in the PSW and PWW. *Actinomma l. leptodermum* and *Actinomma boreale* had been reported previously as forming a taxonomic group (e.g., Samtleben et al., 1995) due to identification problems, particularly of the juvenile stages. However, the adult stages can be separated into two species following Cortese and Bjørklund (1998). *Actinomma l. leptodermum* were absent in the water masses of SML and PSW at Station 32, but they were abundant in these water masses at Station 56. At Station 56, SML and PSW water masses were colder (-1.2 to 0.6ºC) and more homogeneous than at Station 32; indicating that Actinommidae spp. juvenile forms and *A. l. leptodermum* preferred slightly warmer water than PWW (-1.6ºC). We found that Actinommidae spp. juvenile forms and *A. l. leptodermum* are most abundant in the upper water layers where phytoplankton also prevails (Fig. 2). It is most likely that the juvenile actinommids and *A. l. leptodermum* may be bound to the euphotic zone. *Spongotrochus glacialis* also preferred warmer water than PWW. This species inhabited surface water in the Okhotsk Sea, and is well adapted to temperatures of >0°C and low salinities (Nimmergut and Abelmann 2002). Okazaki et al. (2004) reported *S. glacialis* as a subsurface dweller with abundance maximum in the 50–100 m interval in the Okhotsk Sea, associated with peaks in the phytoplankton production.

5.2.2. PWW association

Joergensenium sp. A, *Pseudodictyophimus clevei*, and *Actinomma boreale,* were mainly distributed in the PWW. *Joergensenium* sp. A and *P. clevei* might prefer cold water (-1.7°C) with low turbulence. The depth distribution of *Joergensenium* sp. A was restricted to the PWW (100-250 m) and the upper AW (250-500 m), but *P. clevei* was more widely distributed. *Joergensenium* sp. A has not yet been described from recent radiolarian assemblages, so it can be suggested that this species might occur only on the Pacific side of the Arctic Ocean, and might serve as an indicator for the PWW layer. Abundance of *A. boreale* was lower than Actinommidae spp. juvenile forms and *A. l. leptodermum* at both stations, and mainly occurred in the PWW. In the surface sediments of the Greenland, Iceland and Norwegian Seas, *A. boreale* is associated with warm (Atlantic) water, whereas *A. l. leptodermum* seems to have broader environmental tolerance, as it is associated with both the cold East Greenland Current and the warm Norwegian Current water (Bjørklund et al., 1998). Other environmental factors such as salinity, food availability, or seasonal differences of their growth stages due to the sampling period might influence the standing stocks of *A. boreale*.

5.2.3. Upper AW association

Ceratocyrtis histricosus was not found in the Canada Basin in 1950's and 1960's, and the common occurrence of this species in the AW in the Chukchi and Beaufort seas in 2000 might be an effect of the recent warming of the AW (Itaki et al., 2003). We also found this species was common in the upper AW and firstly found in the PWW in the western Arctic Ocean in our plankton tow samples collected in 2013. Since the water temperature where this species occurred ranged from −1.6 (this study) to 10ºC (Swanberg and Bjørklund, 1987), slight increase of the temperature in the AW (0.2ºC) and PWW (0.05ºC) in the Arctic Ocean (Swift at al., 1997; McLaughlin et al., 2011) could not be a reason for the expansion of the range of this species. The change of North Atlantic Oscillation (atmospheric High and Low pressure cells) that controls the flow of the surface water in the North Atlantic has sustained the increase of Atlantic inflow in the Arctic Ocean (Zhang et al., 1998). This temporary increasing volumes of inflowing AW might increase the chances for more exotic radiolarians to reach into the Arctic Ocean.

5.2.4. Lower AW association

Pseudodictyophimus plathycephalus, Plagiacanthidae gen. et sp. indet. (Pl. 8, Figs. 11-18), and *Cycladophora davisiana* were abundant in the cold and oxygenated lower AW at both Stations 32 and 56. Although, the distribution patterns of these two species in PWW and upper AW water masses were slightly different between Station 32 and Station 56, the temperature, salinity, and dissolved oxygen were similar at both stations. Their abundance might, therefore, reflect the influence of other variables than hydrographic conditions alone. *Pseudodictyophimus g. gracilipes* is widely distributed in the World Ocean, and inhabits the surface layer at high latitudes, but dwells at greater depths at low latitudes (Ishitani and Takahashi, 2007; Ishitani et al., 2008). Itaki et al. (2003) reported that the maximum depth *P. g. gracilipes* occurred at 0-50 m in the Chukchi Sea, and 25-50 m in the Beaufort Sea. However, in our results, *P. g. gracilipes* did not show any specific vertical distribution, and its abundance was low.

5.3. Seasonal and annual radiolarian flux

5.3.1. Radiolarian fauna and seasonal sea-ice concentration

Seasonal radiolarian fluxes at Station NAP were characterized by the high dominance of a few species and by the changes of their ratios in the upper trap with the seasonal changes in sea-ice concentration. *Amphimelissa setosa* adult and its juvenile forms were dominant during the open-water season and around the beginning and the end of ice-cover seasons, while the actinommids (Actinommidae spp. juvenile forms, *Actinomma l. leptodermum*, and *Actinomma boreale*) were dominant during the ice-cover season (Fig. 5). These observations might explain the regional difference in the radiolarian species distribution in the Arctic Ocean. *Amphimelissa setosa* were dominant in Arctic marginal sea sediments (Iceland, Barents, and Chukchi Seas) where sea ice disappeared in the summer, but Actinommidae were dominant in the central Arctic Ocean (Nansen, Amundsen, and Makarov Basins) where the sea surface was covered by sea ice throughout the year (Bjørklund and Kruglikova, 2003). Zasko et al. (2014) also reported that *A. setosa* was essentially absent in the plankton samples in the central polar basins.

The summer ice edge hosts well-grown ice algae and ice fauna (Horner et al., 1992; Michel et al., 2002; Assmy et al., 2013), and the summer ice edge causes an alternation between stable water masses and deep vertical mixing where the nutrients are brought to the surface (Harrison and Cota, 1991), with both conditions being favorable for primary

productivity. Swanberg and Eide (1992) found that abundance of *A. setosa* and its juveniles was correlated well with chlorophyll *a* and phaeopigments along the ice edge in summer in the Greenland Sea. Dolan et al. (2014), however, reported that the abundance of *A. setosa* was not always related to high chlorophyll *a* in locales with low sea-ice concentration, as we also have found. Therefore, we interpreted that a cold and well mixed water mass along summer ice edge were essential for high reproduction and growth of *A. setosa*.

From the upper trap, a flux peak of *A. setosa* juveniles occurred at the end of the sea-ice season, and that the flux peak of adult *A. setosa* occurred at the beginning of the sea-ice season (Fig. 7). The time interval between these peaks might indicate that *A. setosa* has a three months life cycle. *Pseudodictyophimus clevei* also shows flux peaks during the beginning of the sea-ice season (November-December) (Fig. 7). These two species seem to prefer to live in a cold water mass with sea-ice formation. On the contrary, juvenile stages of actinommids were dominant during the ice-cover season (Fig. 5). Therefore, we interpreted the actinommids to be tolerant of oligotrophic conditions and are able to live in stratified cold water masses. Itaki and Bjørklund (2007) reported that reproduction could occur even during the juvenile stage in at least some actinommids, because they frequently found conjoined juvenile Actinommidae skeletons in the Japan Sea sediments. Furthermore, the flux of Actinommidae spp. juvenile forms increased towards the end of the sea-ice cover season, accompanied by an increase in downward shortwave radiation (Fig. 5 and 7). This might indicate that the Actinommidae spp. juvenile form can feed on algae growing on the ice, or prey on other phytoplankton under the sea ice.

This study showed that the productivity of radiolarians was high, but diversity was low, during summer season with low sea-ice concentration in the western Arctic Ocean (Fig. 5 and 6). In contrast, radiolarian fauna in the sediment trap that was moored in the Okhotsk Sea showed high diversity during the summer season (Okazaki et al., 2003). The maximum total radiolarian flux during the summer season around the sea-ice edge and the open water is characterized by high dominance of *A. setosa* (>90%) in our sampling area. Such high dominance of a single species does not occur in the Okhotsk Sea, where the main nine taxa contributed to more than 60% of the radiolarian assemblage (Okazaki et al., 2003). *Amphimelissa setosa*, which has a small and delicate siliceous skeleton, might respond directly and rapidly to the changes of water mass

conditions near the summer ice edge. The contrast of seasonal diversity between these two areas seems to be due to the differences in the species composition and in their responses to water mass changes that may differ between these two areas..

Relatively higher fluxes of *Actinomma boreale*, *Spongotrochus glacialis*, and *Joergensenium* sp. A during the sea-ice free season in the upper trap in summer of 2012 compared to summer of 2011 might be due to the deeper mooring depth of the upper trap after October 2011 (Fig. 7 and S1); because, in general, these three species are more abundant at depths deeper than the first upper trap depth at about 180 m (Fig. 3a). Although, *Ceratocyrtis histricosus* and *Tripodiscium gephyristes* were mainly distributed in deeper depths (>250 m) than the upper trap depth (Fig. 4), flux of these two species in the upper trap apparently increased in the summer of 2012. The water temperature at the upper trap increased during this period (Fig. 7 and S1). We, therefore, interpreted this increase of *Ceratocyrtis histricosus* and *Tripodiscium gephyristes* to be related to the mixing of the nutrient-rich and warm upper AW with the lower PWW.

5.3.2. Radiolarian fauna and interannual difference in ocean circulation

Intensification of geostrophic currents on the periphery of the Beaufort Gyre (Fig. 1) has been reported in recent years (Nishino et al., 2011; McPhee, 2013). This intensification is caused by an increasing volume of water from melting sea ice in association with the reduction of arctic summer sea ice and the river runoff to the basins (Proshutinsky et al., 2009; Yamamoto-Kawai et al., 2008). The total radiolarian flux during summer (July-September) was lower in 2012 than in 2011 in both the upper and lower traps (Fig. 5). Flux of most radiolarian taxa was also lower during summer of 2012 (Fig. 7). On the other hand, fluxes of the actinommids (Actinommidae spp. juvenile forms, *Actinomma l. leptodermum*, and *Actinomma boreale*), possibly adapted to cold and oligotrophic water, was greater during December 2011-September 2012 than during December 2010-September 2011. Actinommidae spp. juvenile forms and *A. l. leptodermum* were most abundant in the depth interval of 0-100 m at Station 56 in the southwestern Canada Basin. Therefore, we suspected that the cold and oligotrophic water in the Canada Basin began to spread to Station NAP in the Northwind Abyssal Plain from December 2011, and continued to affect the radiolarian fluxes at least until September 2012. McLaughlin et al. (2011) reported that the position of the center of the Beaufort Gyre shifted westwards, and that the area influenced by the gyre has spread

northwards and westwards in recent years. Moreover, the high-resolution pan-Arctic Ocean model results also showed that the Beaufort Gyre expanded by shifting its center from the Canada Basin interior to the Chukchi Borderland in 2012 compared with 2011; and the ocean current direction in the surface 100 m layer switched northwestward to southwestward in December 2011 (E. Watanabe, personal communication, 2014). Thus, recent intensification of Beaufort Gyre currents associated with sea-ice reduction, would have affected the surface water mass conditions and as well as the ecological conditions in the western Arctic Ocean.

5.3.3. Vertical and lateral transport

Flux peaks of total radiolarians in the lower trap are delayed by about two weeks in comparison to the upper trap (Fig. 5). Therefore, the sinking speed of the aggregated radiolarian particle flux between these depths were averaged to 74 m day^{-1} during November-December 2010, 86 m day^{-1} during July-August 2011, and 73 m day^{-1} during November 2011. Watanabe et al. (2014) simulated movement of cold and warm eddies using a high-resolution pan-Arctic Ocean model, and suggested that the high total mass flux during October-December 2010 at Station NAP, as we found, was mainly due to the enhancement of the marine biological pump by an anti-cyclonic cold eddy. Shelf-break eddies induce the lateral transport of re-suspended bottom sediments composed of old carbon, and enhance the biological pump (O'Brien et al., 2013; Watanabe et al., 2014). Actually, the passage of a cold eddy was observed as a cooling and a deepening of the moored trap depth in the corresponding period (Fig. S1). *Amphimelissa setosa* was the most dominant species (>90%) and showed the highest flux (13,840 specimens m^{-2} day^{-1}) during November 2010 in the upper trap. The flux of this species during November 2010 in the upper trap was about 3,500 specimens m^{-2} day^{-1} higher than that in 2011 and kept a highest value half a month longer than that in 2011. The cold eddy passage would transport a cold and well mixed water mass, conditions favorable for *A. setosa*. Therefore, the cold eddy passage, in addition to seasonal water mass variations with sea ice formation, would enhance the high radiolarian flux.

Radiolarian fluxes in the lower trap were generally higher than in the upper trap, except for May-September 2012 (Fig. 5). The extremely low fluxes in the lower trap during this interval might be due to a decrease of aggregate formation. The latter

process, which helps rapid sinking of biogenic particles, would be suppressed by influx of oligotrophic surface water originating from the Beaufort Gyre in the Canada Basin. In the southwestern Canada Basin (Station 56), high standing stock of dead radiolarian specimens (Fig. 2) might indicate an inefficient biological pump in this area. In addition, fluxes of Actinommidae spp. juvenile forms were lower in the lower trap, in spite of their high abundance in the upper trap since December 2011. We suggest that the disappearance of fluxes of Actinommidae spp. juvenile forms in the lower trap might be due to lack of aggregate formation.

Higher abundance in the lower trap of species having a wider vertical distribution (*Pseudodictyophimus g. gracilipes*, *P. plathycephalus*) or intermediate to deep water distribution (*Ceratocyrtis histricosus, Tripodiscium gephyristes*, Plagiacanthidae gen. et sp. indet., and *Cycladophora davisiana*) might be attributed to the reproduction of these species at a depth level situated between the upper and lower traps. The flux of *Pseudodictyophimus g. gracilipes*, *P. plathycephalus*, Plagiacanthidae gen. et sp. in det. and *Cycladophora davisiana* in the lower trap was high during July-August 2011. The flux of most of the radiolarian species in the lower trap also peaked during March 2011, a period of heavy ice cover and low downward shortwave radiation. In addition, in the lower trap the flux peak during March in 2011 was made up of more than 80% of *A. setosa*, a definite surface water species. However, during this period a similar peak was not found in the upper trap. Therefore, the flux peaks during March 2011 could be derived from some lateral advection at a depth lower than 180 m or a re-suspension of shelf sediments.

Acknowledgements

We are grateful to the captain, officers and crews of the CCGS Sir Wilfrid Laurier, R.V. Mirai (JAMSTEC), operated by GODI, R/V, Dr. Humfrey Melling (IOS, Canada), Dr. Shigeto Nishino for their help in the mooring operation and sampling collection. We are thankful to Dr. A. Matul (P.P. Shirshov Institute of Oceanology, Russian Academy of Sciences, Moscow) for critically reading and commenting on our manuscript. We similarly thankful to G. Cortese for his detailed comments and correcting our English, this greatly improved our manuscript. We are thankful to one anonymous reviewer who had some good and helpful comments and suggestions. We finally acknowledge Dr. O.R. Anderson for reading our manuscript, for his comments and proofing our English.

This work was supported by JSPS KAKENHI Grant Number 22221003 to NH and JSPS KAKENHI Grant Number 24•4155 and 26740006 to TI. TI received partial fund from Tatsuro Matsumoto Scholarship Fund of the Kyushu University. This work was partly carried out when TI was visiting the Natural History Museum, University of Oslo in 2013.

References

Aagaard, K., Coachman, L. K., and Carmack, E.: On the halocline of the Arctic Ocean, Deep-Sea Res. Pt. I, 28, 529–545, 1981.

Aagaard, K., Swift, J. H., and Carmack, E. C.: Thermohaline circulation in the Arctic Mediterranean seas, J. Geophys. Res., 90, 4833–4846, 1985.

Adl, S. M., Simpson, G. B., Farmer, M. A., Andersen, R. A., Anderson, O. R., Barta, J. R., Bowser, S. S., Brugerolle, G., Fensome, R. A., Fredericq, S., James, T. Y., Karpov, S., Kugrens, P., Krug, J., Lane, C. E., Lewis, L. A., Lodge, J., Lynn, D. H., Mann, D. G., Mccourt, R. M., Mendoza, L., Moestrup, Ø., Mozley-Standridge, S. E., Nerad, T. A., Shearer, C. A., Smirnov, A. V., Spiegel, F. W., and Taylor, M. F. J. R.: The new higher level classification of Eukaryotes with emphasis on the taxonomy of protists, J. Eukaryot. Microbiol. 52, 399–451, 2005.

Anderson, O. R.: Radiolaria, Springer, New York, 365 pp., 1983.

Arrigo, K. R., Perovich, D. K., Pickart, R. S., Brown, Z. W., van Dijken, G. L., Lowry, K. E., Mills, M. M., Palmer, M. A., Balch, W. M., Bahr, F., Bates, N. R., Benitez-Nelson, C., Bowler, B., Brownlee, E., Ehn, J. K., Frey, K. E., Garley, R., Laney, S. R., Lubelczyk, L., Mathis, J., Matsuoka, A., Mitchell, B. G., Moore, G. W. K., Ortega-Retuerta, E., Pal, S., Polashenski, C. M., Reynolds, R. A., Scheiber, B., Sosik, H. M., Stephens, M., and Swift, J. H.: Massive phytoplankton blooms under Arctic sea ice, Science, 336, 1408, doi:10.1126/science.1215065, 2012.

Assmy, P., Ehn, J. K., Fernández-Méndez, M., Hop, H., Katlein, C., Sundfjord, A., Bluhm, K., Daase, M., Engel, A., Fransson, A., Granskog, M. A., Hudson, S. R., Kristiansen, S., Nicolaus, 5 M., Peeken, I., Renner, A. H. H., Spreen, G., Tatarek, A., and Wiktor, J.: Floating ice–algal aggregates below melting Arctic Sea ice, PLoS ONE, 8, e76599, doi:10.1371/journal.pone.0076599, 2013.

Bailey, J. W.: Notice of microscopic forms found in the soundings of the Sea of Kamtschatka, Am. J. Sci. Arts, 22, 1–6, 1856.

Bates, N. R. and Mathis, J. T.: The Arctic Ocean marine carbon cycle: evaluation of air-sea CO2 exchanges, ocean acidification impacts and potential feedbacks, Biogeosciences, 6, 2433–2459, doi:10.5194/bg-6-2433-2009, 2009.

Bates, N. R., Moran, S. B., Hansell, D. A., and Mathis, J. T.: An increasing CO2 sink in the Arctic Ocean due to sea-ice loss, Geophys. Res. Lett., 33, L23609, doi:10.1029/2006GL027028, 2006.

Bernstein, T.: Protist plankton of the North-west part of the Kara Sea, Transactions of the Arctic Institute, 3, 1–23, 1931 (in Russian with English summary).

Bernstein, T.: Über einige arktische Radiolarien, Arch. Protistenkunde, 76, 217–227, 1932.

Bernstein, T.: Zooplankton des Nordlischen teiles des Karischen Meeres, Transactions of the Arctic Institute, 9, 3–58, 1934 (in Russian with German summary).

Bjørklund, K. R. and Kruglikova, S. B.: Polycystine radiolarians in surface sediments in the Arctic Ocean basins and marginal seas, Mar. Micropaleontol., 49, 231–273, 2003.

Bjørklund, K. R., Cortese, G., Swanberg, N., and Schrader, H. J.: Radiolarian faunal provinces in surface sediments of the Greenland, Iceland and Norwegian (GIN) seas, Mar. Micropaleontol., 35, 105–140, 1998.

Bjørklund, K. R., Dumitrica, P, Dolven, J. K., and Swanberg, N. R.: Joergensenium rotatile n. gen., n. sp. (Entactinaria, Radiolaria): its distribution in west Norwegian fjords, Micropaleontology, 53, 457–468, 2008.

Bjørklund, K. R., Itaki, T., and Dolven, J. K.: Per Theodor Cleve: a short résumé and his radiolarian results from the Swedish Expedition to Spitsbergen in 1898, J. Micropalaeontol., 33, 59–93, 2014.

Boetius, A., Albrecht, S., Bakker, K. B., Bienhold, C., Felden, J., Fernández-Méndez, M., Hendricks, S., Katlein, C., Lalande, C., Krumpen, T., Nicolaus, M., Peeken, I., Rabe, B., Rogacheva, A., Rybakova, E., Somavilla, R., and Wenzhöfer, F.: Export of algal biomass from the melting arctic sea ice, Science, 339, 1430–1432, doi:10.1126/science.1231346, 2013.

Boltovskoy, D., Kling, S. A., Takahashi, K., and Bjørklund, K. R.: World atlas of distribution of recent polycystina (Radiolaria), Palaeontol. Electron., 13, 1–230, available at: http: //palaeo-electronica.org/2010_3/215/index.html (last access: 29 November 2014), 2010.

Burridge, A. K., Bjørklund, K. R., Kruglikova, S. B., and Hammer, Ø.: Inter- and intraspecific morphological variation of four-shelled *Actinomma* taxa (Radiolaria) in polar and subpolar regions, Mar. Micropaleontol., 110, 50–71, 2013.

Calbet, A. and Landry, M. R.: Phytoplankton growth, microzooplankton grazing, and carbon cycling in marine systems, Limnol. Oceanogr., 49, 51–57, 2004.

Cavalier-Smith, T.: A revised six-kingdom system of life, Biol. Rev., 73, 203-266, 1998.

Cavalier-Smith, T.: The phagotrophic origin of eukaryotes and phylogenetic classification of Protozoa, Int. J. Syst. Evol. Micr., 52, 297-354, 2002.

Cavalier-Smith, T. and Chao, E. E. Y.: Phylogeny and classification of phylum Cercozoa (Protozoa), Protist, 154, 341–358, 2003.

Cleve, P. T.: Plankton collected by the Swedish Expedition to Spitzbergen in 1898, Kgl. Svenska Vetensk. Akad. Hand., 32, 1–51, 1899.

Coachman, L. and Barnes, C. A.: The contribution of Bering Sea water to the Arctic Ocean, Arctic, 14, 147–161, 1961.

Coachman, L. K., Aagaard, K., and Tripp, R. B.: Bering Strait: the regional physical oceanography, University of Washington Press, Seattle, 172 pp., 1975.

Comiso, J. C., Parkinson, C. L., Gersten, R., and Stock, L.: Accelerated decline in the Arctic sea ice cover, Geophys. Res. Lett., 35, L01703, doi:10.1029/2007GL031972, 2008.

Cortese, G. and Bjørklund, K. R.: The morphometric variation of *Actinomma boreale* (Radiolaria) in Atlantic boreal waters, Mar. Micropaleontol., 29, 271–282, 1997.

Cortese, G. and Bjørklund, K. R.: The taxonomy of boreal Atlantic Ocean. Actinommida (Radiolaria), Micropaleontology, 44, 149–160, 1998.

Cortese, G., Bjørklund, K. R., and Dolven, J. K.: Polycystine radiolarians in the Greenland–Iceland–Norwegian seas: species and assemblage distribution, Sarsia: North Atlantic Marine Science, 88, 65–88, 2003.

Dolan, J. R., Yang, E. J., Kim, T. W. and Kang, S.-H.: Microzooplankton in a warming Arctic: A comparison of tintinnids and radiolarians from summer 2011 and 2012 in the Chukchi Sea, Acta Protozool., 53, 101–113, 2014.

Dolven, J. K., Bjørklund, K. R., and Itaki, T.: Jørgensen's polycystine radiolarian slide collection and new species, J. Micropalaeontol., 33, 21–58, 2014.

Dumitrica, P.: Cleveiplegma n. gen., a new generic name for the radiolarian species

Rhizoplegma boreale (Cleve, 1899), Revue de Micropaléontologie, 56, 21–25, 2013.
Ehrenberg, C. G.: Über die Bildung der Kreidefelsen und des Kreidemergels durch unsichtbare Organismen, Abhandlungen, Jahre 1838, K. Preuss. Akad. Wiss., Berlin, 59–147, 1838.
Ehrenberg, C. G.: Über das organischen Leben des Meeresgrundes in bis 10 800 und 12 000 Fuss Tiefe, Bericht, Jahre 1854, K. Preuss. Akad. Wiss., Berlin, 54–75, 1854.
Ehrenberg, C. G.: Über die Tiefgrund-Verhältnisse des Oceans am Eingange der Davisstrasse und bei Island, Monatsberichte. Jahre 1861, K. Preuss. Akad. Wiss., Berlin, 275–315, 1862.
Ehrenberg, C. G.: Mikrogeologischen Studien über das kleinste Leben der Meeres-Tiefgrunde aller Zonen und dessen geologischen Einfluss, Abhandlungen, Jahre 1873, K. Preuss. Akad. Wiss., Berlin, 131–399, 1873.
Ehrenberg, C. G.: Fortsetzung der mikrogeologischen Studien als Gesammt-Uebersicht der mikroskopischen Palaontologie gleichartig analysirter Gebirgsarten der Erde, mit specieller Rucksicht auf den Polycystinen-Mergel von Barbados, Abhandlungen, Jahre 1875, K. Preuss. Akad. Wiss., Berlin, 1–225, 1875.
Ewing, M. and Connary, S.: Nepheloid layer in the North Pacific, in: Geological Investigations of the North Pacific, edited by: Hays, J. D., Geol. Soc. Am. Mem., 126, 41–82, 1970.
Francois, R., Honjo, S., Krishfield, R., and Manganini, S.: Factors controlling the flux of organic carbon to the bathypelagic zone of the ocean, Global Biogeochem. Cy., 16, 1087, doi:10.1029/2001GB001722, 2002.
Haeckel, E.: Die Radiolarien (Rhizopoda Radiaria) – Eine Monographie, Reimer, Berlin, 572 pp., 1862.
Haeckel, E.: Über die Phaeodarien, eine neue Gruppe kieselschaliger mariner Rhizopoden, Jenaische Zeitschrift für Naturwissenschaft, 14, 151–157, 1879.
Haeckel, E.: Prodromus Systematis Radiolarium, Entwurf eines Radiolarien-Systems auf Grund von Studien der Challenger-Radiolarien, Jenaische Zeitschrift für Naturwissenschaft,15, 418–472, 1881.
Haeckel, E.: Report on the Radiolaria collected by the H.M.S. *Challenger* during the Years 1873–1876, Report on the Scientific Results of the Voyage of the H.M.S. *Challenger*, Zoology, 18, 1–1803, 1887.
Harrison, W. G. and Cota, G. F.: Primary production in polar waters: relation to nutrient

availability, Polar Res., 10, 87–104, 1991.
Hertwig, R.: Der Organismus der Radiolarien, Jenaische Denkshr., 2, 129–277, 1879.
Honjo, S., Krishfield, R. A., Eglinton, T. I., Manganini, S. J., Kemp, J. N., Doherty, K., Hwang, J., Mckee, T. K., and Takizawa, T.: Biological pump processes in the cryopelagic and hemipelagic Arctic Ocean: Canada Basin and Chukchi Rise, Prog. Oceanogr., 85, 137–170, 2010.
Horner, R. A., Ackley, S. F., Dieckmann, G. S., Gulliksen, B., Hoshiai, T., Legendre, L., Melnikov, I. A., Reeburgh, W. S., Spindler, M., and Sullivan, C. W.: Ecology of sea ice biota. 1. Habitat, terminology, and methodology, Polar Biol., 12, 417–427, 1992.
Hülseman, K.: Radiolaria in plankton from the Arctic drifting station T-3, including the description of three new species, Arc. Inst. North Am. Tech. Pap., 13, 1–52, 1963.
Ikenoue, T., Ishitani, Y., Takahashi, K., and Tanaka, S.: Seasonal flux changes of radiolarians at Station K2 in the Western Subarctic Gyre, Umi no Kenkyu (Oceanography in Japan), 19, 165–185, 2010 (in Japanese, with English abstract).
Ikenoue, T., Takahashi, K., and Tanaka, S.: Fifteen year time-series of radiolarian fluxes and environmental conditions in the Bering Sea and the central subarctic Pacific, 1990–2005, Deep-Sea Res. Pt. II, 61–64, 17–49, 2012a.
Ikenoue, T., Ueno, H., and Takahashi, K.: Rhizoplegma boreale (Radiolaria): a tracer for mesoscale eddies from coastal areas, J. Geophys. Res., 117, C04001, doi:10.1029/2011JC007728, 2012b.
Ishitani, Y. and Takahashi, K.: The vertical distribution of Radiolaria in the waters surrounding Japan, Mar. Micropaleontol., 65, 113–136, 2007.
Ishitani, Y., Takahashi, K., Okazaki, Y., and Tanaka, S.: Vertical and geographic distribution of selected radiolarian species in the North Pacific, Micropaleontology, 54, 27–39, 2008.
Itaki, T. and Bjørklund, K. R.: Conjoined radiolarian skeletons (Actinommidae) from the Japan Sea sediments, Micropaleontology, 53, 371–389, 2007.
Itaki, T., Ito, M., Narita, H., Ahagon, M., and Sakai, I.: Depth distribution of radiolarians from the Chukchi and Beaufort Seas, western Arctic, Deep-Sea Res. Pt. I, 50, 1507–1522, 2003.
Itoh, M., Nishino, S., Kawaguchi, Y., and Kikuchi, T.: Barrow Canyon fluxes of volume, heat and freshwater revealed by mooring observations, J. Geophys. Res., 118, 4363–4379, 2013.

Jackson, J. M., Allen, S. E., McLaughlin, F. A., Woodgate, R. A., and Carmack, E. C.: Changes to the near surface waters in the Canada Basin, Arctic Ocean from 1993–2009: a basin in transition, J. Geophys. Res., 116, C10008, doi:10.1029/2011JC007069, 2011.

Jones, E. P. and Anderson, L. G.: On the origin of the chemical properties of the Arctic Ocean halocline, J. Geophys. Res., 91, 10759–10767, 1986.

Jørgensen, E.: Protophyten und Protozöen im Plankton aus der norwegischen Westküste, Bergens Museumus Aarbog 1899, 6, 51–112, 1900.

Jørgensen, E.: The Protist plankton and the diatoms in bottom samples, Plates VIII–XVIII, Bergens Museuns Skrifter, 1, 49–151, 1905.

Kling, S. A.: Vertical distribution of polycystine radiolarians in the central North Pacific, Mar. Micropaleontol., 4, 295–318, 1979.

Kosobokova, K. N., Hirche, H. -J. and Scherzinger, T.: Feeding ecology of Spinocalanus antarcticus, a mesopelagic copepod with a looped gut, Mar. Biol., 141, 503–511, 2002.

Kozur, H. and Möstler, H.: *Entactinaria subordo* Nov., a new radiolarian suborder, Geologisch Paläontologische Mitteilungen, Innsbruck, 11, 399–414, 1982.

Kruglikova, S. B., Bjørklund, K. R., Hammer, Ø., and Anderson, O. R.: Endemism and speciation in the polycystine radiolarian genus *Actinomma* in the Arctic Ocean: description of two new species *Actinomma georgii* n. sp., and *A. turidae* n. sp., Mar. Micropaleontol., 72, 26–48, 2009.

Kruglikova, S. B., Bjørklund, K. R., Dolven, J. K., Hammer, Ø., and Cortese, G.: High-rank polycystine radiolarian taxa as temperature proxies in the Nordic Seas, Stratigraphy, 7, 265–281, 2010.

Kruglikova, S. B., Bjørklund, K. R., and Hammer, O.: High rank taxa of Polycystina (Radiolaria) as environmental bioindicators, Micropaleontology, 57, 483–489, 2011.

Lovejoy, C. and Potvin, M.: Microbial eukaryotic distribution in a dynamic Beaufort Sea and the Arctic Ocean, J. Plankton Res., 33, 431–444, 2011.

Lovejoy, C., Massana, R., and Pedrós-Alió, C.: Diversity and distribution of marine microbial eukaryotes in the Arctic Ocean and adjacent seas, Appl. Environ. Microb., 72, 3085–3095, doi:10.1128/AEM.72.5.3085-3095.2006, 2006.

Markus, T., Stroeve, J. C., and Miller, J.: Recent changes in Arctic sea ice melt onset, freezeup, and melt season length, J. Geophys. Res., 114, C12024,

doi:10.1029/2009JC005436, 2009.
Matul, A. and Abelmann, A.: Pleistocene and Holocene distribution of the radiolarian *Amphimelissa setosa* Cleve in the North Pacific and North Atlantic: evidence for water mass movement, Deep-Sea Res. Pt. II, 52, 2351–2364, 2005.
McLaughlin, F. A., Carmack, E., Proshutinsky, A., Krishfield, R. A., Guay, C. K., Yamamoto-Kawai, M., Jackson, J. M., and Williams, W. J.: The rapid response of the Canada Basin to climate forcing: From bellwether to alarm bells, Oceanography, 24, 146–159, doi:10.5670/oceanog.2011.66, 2011.
McPhee, M.: Intensification of geostrophic currents in the Canada Basin, Arctic Ocean, J. Climate,26, 3130, doi:10.1175/JCLI-D-12-00289.1, 2013.
Meunier, A.: Microplankton des Mers de Barents et de Kara, Duc d'Orléans, Campagne arctique de 1907, 255 pp., 1907.
Michel, C., Nielsen, T. C., Nozais, C., and Gosselin, M.: Significance of sedimentation and grazing by ice micro- and meiofauna for carbon cycling in annual sea ice (northern Baffin Bay), Aquat. Microb. Ecol., 30, 57–68, 2002.
Murray, J.: The Radiolaria. Narrative of the cruise of the H.M.S. "*Challenger*" with a general account of the scientific results of the expedition, in: Report from the Voyage of the H.M.S. *Challenger*, edited by: Tizard, T. H., Moseley, H. N., Buchanan, J. Y., and Murray, J., Narrative, 1, 219–227, 1885.
Müller, J.: Über die Thalassicollen, Polycystinen und Acanthometren des Mittelmeeres, Abhandlungen, Jahre 1858, K. Preuss. Akad. Wiss., Berlin, 1–62, 1858.
Nikolaev, S. I., Berney, C., Fahrni, J., Bolivar, I., Polet, S., Mylnikov, A. P., Aleshin, V. V., Petrov, N. B., and Pawlowski, J.: The twilight of Heliozoa and rise of Rhizaria, an emerging supergroup of amoeboid eukaryotes, P. Natl. Acad. Sci. USA, 101, 8066–8071, 2004.
Nimmergut, A. and Abelmann, A.: Spatial and seasonal changes of radiolarian standing stocks in the Sea of Okhotsk, Deep-Sea Res. Pt. I, 49, 463–493, 2002.
Nishino, S., Kikuchi, T., Yamamoto-Kawai, M., Kawaguchi, Y., Hirawake, T., and Itoh, M.: Enhancement/reduction of biological pump depends on ocean circulation in the sea-ice reduction regions of the Arctic Ocean, J. Oceanogr., 67, 305–314, doi:10.1007/s10872-011-0030-7, 2011.
Nishino, S.: R/V *Mirai* cruise report MR13-06, 226 pp., available at: www.godac.jamstec.go.jp/darwin/datatree/e (last access: 29 November 2014),

JAMSTEC, Yokosuka, Japan, 2013.

NSIDC (National Snow and Ice Data Center): Arctic sea ice extent settles at record seasonal minimum, available at: http://nsidc.org/arcticseaicenews/2012/09/ (last access: 29 November 2014), 2012.

O'Brien, M. C., Melling, H., Pedersen, T. F., and Macdonald, R.W.: The role of eddies on particle flux in the Canada Basin of the Arctic Ocean, Deep-Sea Res. Pt. I, 71, 1–20, 2013.

Okazaki, Y., Takahashi, K., Yoshitani, H., Nakatsuka, T., Ikehara, M., and Wakatsuchi, M.: Radiolarians under the seasonally sea-ice covered conditions in the Okhotsk Sea: flux and their implications for paleoceanography, Mar. Micropaleontol., 49, 195–230, 2003.

Okazaki, Y., Takahashi, K., Itaki, T., and Kawasaki, Y.: Comparison of radiolarian vertical distributions in the Okhotsk Sea near the Kuril Islands and in the northwestern North Pacific off Hokkaido Island, Mar. Micropaleontol., 51, 257–284, 2004.

Okazaki, Y., Takahashi, K., Onodera, J., and Honda, M. C.: Temporal and spatial flux changes of radiolarians in the northwestern Pacific Ocean during 1997–2000, Deep-Sea Res. Pt. II, 52, 2240–2274, 2005.

Onodera, J., Watanabe, E., Harada, N., and Honda, M. C.: Diatom flux reflects water-mass conditions on the southern Northwind Abyssal Plain, Arctic Ocean, Biogeosciences Discuss., 11, 15215-15250, doi:10.5194/bgd-11-15215-2014, 2014.

Petrushevskaya, M. G.: Radiolarians of orders Spumellaria and Nassellaria of the Antarctic region (from material of the Soviet Antarctic Expedition), in: Studies of Marine Fauna IV(XII): Biological Reports of the Soviet Antarctic Expedition (1955–1958), edited by: Andriyashev, A. P. and Ushakov, P. V., Academy of Sciences of the USSR, Zoological Institute, Leningrad, 3, 2–186, 1967 (translated from Russian and published by Israel Program for Scientific Translations, 1968).

Petrushevskaya, M. G.: Radiolyarii Nassellaria v planktone Mirovogo Okeana, Issledovaniya Fauny Morei, 9, 1–294, 1971 (+ App., 374–397), Nauka, Leningrad, in Russian.

Popofsky, A.: Die Radiolarien der Antarktis (mit Ausnahme der Tripyleen), in: Deutsche Südpolar-Expedition 1901–1903. X, Zoologie, 2, part 3, edited by: Drygalski, E., Georg Reimer, Berlin, 184–305, 1908.

Proshutinsky, A., Bourke, R. H., and McLaughlin, F. A.: The role of the Beaufort Gyre in Arctic climate variability: seasonal to decadal climate scales, Geophys. Res. Lett., 29, 2100, doi:10.1029/2002GL015847, 2002.

Proshutinsky, A., Krishfield, R., Timmermans, M. L., Toole, J., Carmack, E., McLaughlin, F., Williams, W. J., Zimmermann, S., Itoh, M., and Shimada, K.: Beaufort Gyre freshwater reservoir: state and variability from observations, J. Geophys. Res., 114, C00A10, doi:10.1029/2008JC005104, 2009.

Reynolds, R. W., Rayner, N. A., Smith, T. M., Stokes, D. C., and Wang, W.: An improved in situ and satellite SST analysis for climate, J. Climate, 15, 1609–1625, 2002.

Riedel, W. R.: Subclass radiolaria, in: The Fossil Record, edited by: Harland, W. B. et al., Geol. Soc. London, London, UK, 291–298, 1967.

Saha, S., Moorthi, S., Pan, H. L., Wu, X. R., Wang, J. D., Nadiga, S., Tripp, P., Kistler, R., Woollen, J., Behringer, D., Liu, H. X., Stokes, D., Grumbine, R., Gayno, G., Wang, J., Hou, Y. T., Chuang, H. Y., Juang, H. M. H., Sela, J., Iredell, M., Treadon, R., Kleist, D., Van Delst, P., Keyser, D., Derber, J., Ek, M., Meng, J., Wei, H. L., Yang, R. Q., Lord, S., Van den Dool, H., Kumar, A., Wang, W. Q., Long, C., Chelliah, M., Xue, Y., Huang, B. Y., Schemm, J. K., Ebisuzaki, W., Lin, R., Xie, P. P., Chen, M. Y., Zhou, S. T., Higgins, W., Zou, C. Z., Liu, Q. H., Chen, Y., Han, Y., Cucurull, L., Reynolds, R. W., Rutledge, G., and Goldberg, M.: The NCEP climate forecast system reanalysis, B. Am. Meteorol. Soc., 91, 1015–1057, 2010.

Samtleben, C., Schäfer, P., Andruleit, H., Baumann, A., Baumann, K. H., Kohly, A., Matthiessen, J., and Schröder-Ritzrau, A.: Plankton in the Norwegian–Greenland Sea: from living communities to sediment assemblages – an actualistic approach, Geol. Rundsch., 84, 108–136, 1995.

Shannon, C. E. and Weaver, W.: The Mathematical Theory of Communication, University of Illinois Press, Urbana, 125 pp., 1949.

Shimada, K., Carmack, E. C., Hatakeyama, K., and Takizawa, T.: Varieties of shallow temperature maximum waters in the western Canadian Basin of the Arctic Ocean, Geophys. Res. Lett., 28, 3441–3444, 2001.

Shimada, K., Kamoshida, T., Itoh, M., Nishino, S., Carmack, E., McLaughlin, F., Zimmermann, S., and Proshutinsky, A.: Pacific Ocean inflow: influence on catastrophic reduction of sea ice cover in the Arctic Ocean, Geophys. Res. Lett., 33,

L08605, doi:10.1029/2005GL025624, 2006.
Stroeve, J., Holland, M. M., Meier, W., Scambos, T., and Serreze, M.: Arctic sea ice decline: faster than forecast, Geophys. Res. Lett., 34, L09501, doi:10.1029/2007GL029703, 2007.
Stroeve, J. C., Serreze, M. C., Holland, M. M., Kay, J. E., Malanik, J., and Barrett, A. P.: The Arctic's rapidly shrinking sea ice cover: a research synthesis, Climatic Change, 110, 1005–1027, doi:10.1007/s10584-011-0101-1, 2012.
Suzuki N. and Aita Y.: Achievement and unsolved issues on radiolarian studies: Taxonomy and cytology, Plank. Benth. Res., 6, 69–91, 2011.
Swanberg, N. R., and Bjørklund, K. R.: Radiolaria in the plankton of some fjords in western and northern Norway: the distribution of species, Sarsia, 72, 231-244, 1987.
Swanberg, N. R. and Eide, L. K.: The radiolarian fauna at the ice edge in the Greenland Sea during summer, 1988, J. Mar. Res., 50, 297–320, 1992.
Swift, J. H., Jones, E. P., Aagaard, K., Carmack, E. C., Hingston, M., Macdonald, R. W., McLaughlin, F. A., and Perkin, R. G.: Waters of the Makarov and Canada basins, Deep-Sea Res. Pt. II, 44, 1503–1529, 1997.
Takahashi, K.: Radiolaria: flux, ecology, and taxonomy in the Pacific and Atlantic, in:, Ocean Biocoenosis, Ser. 3, edited by: Honjo, S., Woods Hole Oceanographic Institution Press, Woods Hole, MA, 303 pp., 1991.
Takahashi, K. and Honjo, S.: Vertical flux of Radiolaria: a taxon-quantitative sediment trap study from the western tropical Atlantic, Micropaleontology, 27, 140–190, 1981.
Tibbs, J. F.: On some planktonic Protozoa taken from the track of Drift Station Arlis I, 1960–1961, J. Arct. Inst. N. Am., 20, 247–254, 1967.
Watanabe, E., Onodera, J., Harada, N., Honda, M. C., Kimoto, K., Kikuchi, T., Nishino, S., Matsuno, K., Yamaguchi, A., Ishida, A., and Kishi, M. J.: Enhanced role of eddies in the Arctic marine biological pump, Nat. Commun., 5, 3950, doi:10.1038/ncomms4950, 2014.
Welling, L. A.: Environmental control of radiolarian abundance in the central equatorial Pacific and implications for paleoceanographic reconstructions, Ph.D. thesis, Oregon State Univ., Corvallis, 314 pp., 1996.
Yamamoto-Kawai, M., McLaughlin, F. A., Carmack, E. C., Nishino, S., and Shimada, K.: Freshwater budget of the Canada Basin, Arctic Ocean, from salinity, _18O, and

nutrients, J. Geophys. Res., 113, C01007, doi:10.1029/2006JC003858, 2008.
Yang, J.: Seasonal and interannual variability of downwelling in the Beaufort Sea, J. Geophys. Res., 114, C00A14, doi:10.1029/2008JC005084, 2009.
Yuasa, T., Takahashi, O., Honda, D., and Mayama, S.: Phylogenetic analyses of the polycystine Radiolaria based on the 18s rDNA sequences of the Spumellarida and the Nassellarida, Eur. J. Protistol., 41, 287–298, 2005.
Zhang, J., Rothrock, D. A., and Steele, M.: Warming of the Arctic Ocean by a strengthened Atlantic inflow: Model results, Geophys. Res. Lett., 25, 1745-1748, 1998.

Table captions

Table 1. Logistic and sample information for the vertical plankton tows for radiolarian standing stock (S. S.) at two stations during R/V *Mirai* Cruise MR13-06

Table 2. Locations, mooring depths, standard sampling interval, and sampled duration of the sediment trap station in the western Arctic Ocean. *Details of the exact durations for each sample are shown in tables S3 and S4.

Table 3. List of 51 radiolarian taxa encountered in the plankton tow and sediment trap samples. All taxa are found in the trap, and * refers to taxa found in trap only.

Supplement table captions

Table S1. Radiolarian counts of living and dead specimens (45μm-1 mm) in plankton tows at Station 32

Table S2. Radiolarian counts of living and dead specimens (45μm-1 mm) in plankton tows at Station 56

Table S3. Radiolarian counts (45μm-1 mm) in upper trap at Station NAP

Table S4. Radiolarian counts (45μm-1 mm) in lower trap at Station NAP

Table S5. Summary information of previous sediment trap studies in the North Pacific Ocean

Figure captions

Fig. 1. Map of the Chukchi and Beaufort Seas showing the locations of sediment traps (solid triangle) and plankton tows (solid circles). Gray arrows indicate the cyclonic circulation of the Beaufort Gyre and the inflow of Pacific water through the Bering

Strait, respectively.

Fig. 2. Depth distributions of total dead and living radiolarians at stations 32 (a), and 56 (b) in comparison to vertical profiles of temperature, salinity, dissolved oxygen, and chlorophyll *a* (Nishino, 2013), and living radiolarian diversity index (Shannon and Weaver, 1949). The different water masses are identified as: Surface Mixed Layer (SML), Pacific Summer Water (PSW), Pacific Winter Water (PWW), Atlantic Water (AW), and Canada Basin Deep Water (CBDW).

Fig. 3. Compositions of living radiolarian assemblages in plankton samples through the upper 1000 m of the water columns at stations 32 (Northwind Abyssal Plain) (a) and 56 (southwestern Canada basin) (b).

Fig. 4. Depth distributions of fourteen living radiolarians in plankton samples at stations 32 (a) and 56 (b).

Fig. 5. (a) Total radiolarian fluxes, diversity index and sea-ice concentration in upper trap at Station NAP. Two samples with fewer than 100 specimens are marked with an asterisk. Sea-ice concentration data are from Reynolds et al. (2002) (http://iridl.ldeo.columbia.edu/SOURCES/.IGOSS/.nmc/.Reyn_SmithOIv2/). (b) Radiolarian faunal compositions in upper trap at Station NAP. (c) Downward short wave radiation at the surface of sea ice and ocean (after sea-ice opening) around Station NAP from National Centers for Environmental Prediction-Climate Forecast System Reanalysis (NCEP-CFSR) (Saha et al., 2010). (d) Total radiolarian fluxes and Shannon-Weaver diversity index in the lower trap at Station NAP. Thirteen samples with fewer than 100 specimens are marked with an asterisk. (e) Radiolarian faunal compositions in lower trap at Station NAP. Barren area: no samples due to trap failure.

Fig. 6. Scatter plots of diversity indices and total radiolarian fluxes at upper (a) and lower trap (b). In these plots, samples with fewer than 100 specimens were excluded.

Fig. 7. Two-year fluxes of major radiolarian taxa at Station NAP during the sampling period.

Fig. 8. Box plot of total radiolarian fluxes at Station NAP and previous studied areas in the North Pacific Ocean (Okazaki et al., 2003, 2005; Ikenoue et al., 2010, 2012a). Summary information of previous sediment trap studies in the North Pacific Ocean is shown in table S5.

Supplement figure caption

Fig. S1. Moored trap depth and the water temperature in the upper trap.

Plate lists

Plate 1. 1–4. *Actinomma boreale* (Cleve, 1899). 1, 2. *Actinomma boreale,* same specimen. NAP10t Shallow #23. 3, 4. *Actinomma boreale,* same specimen. NAP10t Shallow #24. 5–10. *Actinomma leptodermum leptodermum* (Jørgensen, 1900). 5, 6. *Actinomma leptodermum leptodermum,* same specimen. NAP10t Deep #12. 7, 8. *Actinomma leptodermum leptodermum,* same specimen. NAP10t Deep #12. 9, 10. *Actinomma leptodermum leptodermum,* same specimen. NAP10t Deep #12. 11–14. *Actinomma* morphogroup A. 11, 12. *Actinomma* morphogroup A, same specimen. NAP10t Deep #4. 13, 14. *Actinomma* morphogroup A, same specimen. NAP10t Deep #4. 15–18. *Actinomma leptodermum* (Jørgensen, 1900) *longispinum* (Cortese and Bjørklund, 1998). 15, 16. *Actinomma leptodermum longispinum,* same specimen. NAP10t Deep #12. 17, 18. *Actinomma leptodermum longispinum* juvenile, same specimen. NAP10t Deep #12. 19–24. Actinommidae spp. juvenile forms. 19, 20. *Actinomma* sp. indet., same specimen. NAP10t Deep #12. 21, 22. *Actinomma* sp. indet., same specimen. NAP10t Deep #12. 23, 24. *Actinomma* sp. indet., same specimen. NAP10t Deep #12. 25–26. *Actinomma turidae* (Kruglikova and Bjørklund, 2009), same specimen. NAP10t Deep #22.
Scale bar = 100 μm for all figures.

Plate 2. 1–4. *Actinomma* morphogroup B. 1, 2. *Actinomma* morphogroup B, same specimen. NAP10t Deep #4. 3, 4. *Actinomma* morphogroup B juvenile, same specimen. NAP10t Deep #15. 5, 6. *Drymyomma elegans* (Jørgensen, 1900), same specimen. NAP10t Deep #14. 7–9. *Actinomma friedrichdreyeri* (Burridge, Bjørklund and Kruglikova, 2013), same specimen. NAP11t Deep #4. 10–11. *Cleveiplegma boreale* (Cleve, 1899), same specimen. NAP11t Deep #12.
Scale bar = 100 μm for all figures.

Plate 3. 1–4. *Arachnosphaera dichotoma* (Jørgensen, 1900). 1, 2. *Arachnosphaera dichotoma,* same specimen. NAP11t Deep #5. 3, 4. *Arachnosphaera dichotoma,* same specimen. NAP11t Deep #4. 5–8. *Streblacantha circumtexta*? (Jørgensen, 1905). 5, 6. *Streblacantha circumtexta*? juvenile form, same specimen NAP10t Deep #12. 7, 8.

Streblacantha circumtexta? Juvenile form, same specimen. NAP10t Shallow #23. 9–11. *Spongotrochus glacialis* (Popofsky, 1908). 9. *Spongotrochus* aff. *glacialis*. NAP10t Shallow #24. 10, 11. *Spongotrochus glacialis,* same specimen. NAP10t Shallow #22. 12. *Stylodictya* sp. NAP10t Shallow #16.
Scale bar = 100 μm for all figures.

Plate 4. 1–7. *Joergensenium* spp. 1, 2, 3. *Joergensenium* sp. A, same specimen. NAP10t Deep #12. 4, 5. *Joergensenium* sp. A, juvenile forms of 1–3, same specimen. NAP11t Deep #4. 6, 7. *Joergensenium* sp. B, same specimen. NAP11t Deep #9. 8–9. *Enneaphormis rotula* (Haeckel, 1881), same specimen. NAP11t Deep #4. 10–11. *Enneaphormis enneastrum* (Haeckel, 1887), same specimen. NAP10t Deep #12. 12–16. *Protoscenium simplex* (Cleve, 1899). 12, 13, 14. *Protoscenium simplex,* same specimen. NAP10t Deep #12. 15, 16. *Protoscenium simplex,* same specimen. NAP10t Deep #12.
Scale bar = 100 μm for all figures.

Plate 5. 1–6. *Ceratocyrtis histricosus* (Jørgensen, 1905). 1, 2, 3. *Ceratocyrtis histricosus,* same specimen. NAP10t Deep #12. 4, 5, 6. *Ceratocyrtis histricosus,* same specimen. NAP10t Deep #12. 7–10. *Ceratocyrtis galeus* (Cleve, 1899). 7, 8. *Ceratocyrtis galeus,* same specimen. NAP10t Deep #6. 9, 10. *Ceratocyrtis galeus*, same specimen. NAP10t Deep #4. 11–12. *Arachnocorys umbellifera* (Haeckel, 1862), same specimen apical view. NAP10t Deep #4. 13–16. *Cladoscenium tricolpium* (Haeckel, 1887). 13, 14. *Cladoscenium tricolpium*, same specimen. NAP10t Deep #6. 15, 16. *Cladoscenium tricolpium*?, same specimen. NAP10t Deep #14. 17–18. *Lophophaena clevei* (Petrushevskaya, 1971), same specimen. NAP10t Shallow #14. 19–27. *Phormacantha hystrix* (Jørgensen, 1900). 19, 20. *Phormacantha hystrix*, same specimen. NAP10t Deep #12. 21, 22. *Phormacantha hystrix*, same specimen. NAP10t Deep #12. 23, 24, 25. *Phormacantha hystrix*, same specimen. NAP10t Deep #12. 26, 27. *Phormacantha hystrix*, same specimen. NAP10t Deep #12.
Scale bar = 100 μm for all figures.

Plate 6. 1–4. *Peridium longispinum*? (Jørgensen, 1900). 1, 2. *Peridium longispinum*?, same specimen. NAP11t Deep #4. 3, 4. *Peridium longispinum*?, same specimen. NAP11t Deep #4. 5–6. *Plectacantha oikiskos* (Jørgensen, 1905), same specimen.

NAP10t Deep #12. 7–11. *Pseudodictyophimus clevei* (Jørgensen, 1900). 7, 8, 9. *Pseudodictyophimus clevei*, same specimen. NAP10t Deep #12. 10, 11. *Pseudodictyophimus clevei*, same specimen. NAP10t Deep #12. 12–13. *Pseudodictyophimus gracilipes gracilipes* (Bailey, 1856), same specimen. NAP10t Deep #12. 14–19. *Pseudodictyophimus* spp. juvenile forms. 14, 15. *Pseudodictyophimus* indet., juvenile forms same specimen. NAP10t Deep #12. 16, 17. *Pseudodictyophimus* indet., juvenile forms, same specimen. NAP10t Deep #12. 18, 19. *Pseudodictyophimus* indet., juvenile forms same specimen. NAP10t Deep #12. 20–23. *Pseudodictyophimus gracilipes* (Bailey, 1856) *bicornis* (Ehrenberg, 1862). 20, 21. *Pseudodictyophimus gracilipes bicornis*, same specimen. NAP11t Deep #4. 22, 23. *Pseudodictyophimus gracilipes bicornis*, same specimen. NAP11t Deep #4.
Scale bar = 100 μm for all figures.

Plate 7. 1–3. *Pseudodictyophimus gracilipes* (Bailey, 1856) *multispinus* (Bernstein, 1934) 1, 2. *Pseudodictyophimus gracilipes multispinus*, same specimen. NAP10t Shallow #2. 3. *Pseudodictyophimus gracilipes multispinus.* NAP11t Shallow #2. 4–12. *Pseudodictyophimus plathycephalus* (Haeckel, 1887). 4, 5, 6. *Pseudodictyophimus plathycephalus,* same specimen. NAP10t Deep #12. 7, 8. *Pseudodictyophimus plathycephalus,* same specimen. NAP10t Deep #12. 9, 10. *Pseudodictyophimus plathycephalus,* same specimen. NAP10t Deep #12. 11, 12. *Pseudodictyophimus plathycephalus,* same specimen. NAP11t Deep #4. 13–14. *Tetraplecta pinigera* (Haeckel, 1887), same specimen. NAP10t Deep #12.
Scale bar = 100 μm for all figures.

Plate 8. 1–10. *Tripodiscium gephyristes* (Hülsemann, 1963). 1, 2. *Tripodiscium gephyristes*, same specimen. NAP10t Deep #12. 3, 4, 5 *Tripodiscium gephyristes*, same specimen. NAP10t Deep #12. 6, 7, 8. *Tripodiscium gephyristes*, same specimen. NAP10t Deep #12. 9, 10. *Tripodiscium gephyristes*, same specimen. NAP10t Deep #12. 11–18. Plagiacanthidae gen. et sp. indet. 11, 12. Plagiacanthidae gen. et sp. indet. juvenile, same specimen. NAP10t Deep #12. 13, 14. Plagiacanthidae gen. et sp. indet., same specimen. NAP10t Deep #12. 15, 16. Plagiacanthidae gen. et sp. indet., same specimen. NAP10t Deep #12. 17, 18. Plagiacanthidae gen. et sp. indet. juvenile, same specimen. NAP10t Deep #12. 19–22. *Artostrobus annulatus* (Bailey, 1856). 19, 20.

Artostrobus annulatus, same specimen. NAP10t Deep #12. 21, 22. *Artostrobus annulatus*, same specimen. NAP10t Deep #12. 23–30. *Artostrobus joergenseni* (Petrushevskaya, 1967). 23, 24. *Artostrobus joergenseni*, same specimen. NAP10t Deep #12. 25, 26. *Artostrobus joergenseni*, same specimen. NAP10t Deep #12. 27, 28. *Artostrobus joergenseni*, same specimen. NAP10t Deep #12. 29, 30. *Artostrobus joergenseni*, same specimen. NAP10t Deep #12.
Scale bar = 100 μm for all figures.

Plate 9. 1, 2. *Cornutella stylophaena* (Ehrenberg, 1854), same specimen. NAP10t Deep #12. 3, 4. *Cornutella longiseta* (Ehrenberg, 1854), same specimen. NAP10t Deep #12. 5–9. *Cycladophora davisiana* (Ehrenberg, 1862). 5. *Cycladophora davisiana*, NAP11t Deep #4. 6, 7. *Cycladophora davisiana*, same specimen. NAP10t Deep #12. 8, 9. *Cycladophora davisiana*, same specimen. NAP10t Deep #12. 10–11. *Lithocampe a_. furcaspiculata* (Popofsky, 1908). same specimen. NAP10t Deep #12. 12–13. *Lithocampe platycephala* (Ehrenberg, 1873). 12. *Lithocampe platycephala*. NAP10t Deep #13. 13. *Lithocampe platycephala*. NAP11t Deep #14. 14–21. *Sethoconus tabulatus* (Ehrenberg, 1873). 14, 15. *Sethoconus tabulatus*, same specimen. NAP10t Deep #12. 16, 17. *Sethoconus tabulatus*, same specimen. NAP10t Deep #12. 18, 19. *Sethoconus tabulatus*, same specimen. NAP10t Deep #12. 20, 21. *Sethoconus tabulatus*, same specimen. NAP10t Deep #12. 22–33. *Amphimelissa setosa* (Cleve, 1899). 22, 23. *Amphimelissa setosa*, same specimen. NAP10t Deep #12. 24, 25. *Amphimelissa setosa*, same specimen. NAP10t Deep #12. 26, 27. *Amphimelissa setosa*, same specimen. NAP10t Deep #12. 28, 29. *Amphimelissa setosa*, same specimen. NAP11t Deep #4. 30, 31. *Amphimelissa setosa*, same specimen. NAP10t Deep #12. 32, 33. *Amphimelissa setosa*, same specimen, apical view. NAP11t Deep #4. 34–39. *Amphimelissa setosa* juvenile. 34, 35. *Amphimelissa setosa* juvenile, same specimen. NAP11t Deep #14. 36, 37. *Amphimelissa setosa* juvenile, same specimen. NAP10t Deep #12. 38, 39. *Amphimelissa setosa* juvenile, same specimen. NAP11t Deep #14. 40–41. *Lirella melo* (Cleve, 1899), same specimen. NAP10t Deep #14. 42–43. *Protocystis harstoni* (Murray, 1885), same specimen. NAP10t Deep #18.
Scale bar = 100 μm for all figures.

Table 1. Logistic and sample information for the vertical plankton tows for radiolarian standing stock (S. S.) at two stations during R/V Mirai Cruise MR13-06

Station ID		Sampling time (UTC)	Depth interval (m)	Flow water mass (m3)	Aliquot size	Living radiolarian S. S. (count)	Dead radiolarian S. S. (count)	Total radiolarian S. S. (count)
Station 32	74°32' N, 161°54'W	1:24	0-100	20.4	1/4	247 (1257)	75 (381)	322 (1638)
		1:22	100-250	27.2	1/4	96 (654)	116 (790)	212 (1444)
Date	09 Sep 2013	1:18	250-500	39.7	1/2	11 (215)	20 (397)	31 (612)
		1:10	500-1000	79.3	1/2	12 (462)	17 (665)	29 (1127)
Station 56	73°48' N, 159°59'W	17:36	0-100	15.8	1/4	499 (1968)	677 (2671)	1176 (4639)
		17:34	100-250	23.8	1/2	265 (3156)	480 (5711)	745 (8867)
Date	27 Sep 2013	17:30	250-500	40.8	1/2	55 (1125)	276 (5627)	331 (6752)
		17:22	500-1000	81.8	1/2	25 (1034)	83 (3381)	108 (4415)

Table 2. Locations, mooring depths, standard sampling interval, and sampled duration of the sediment trap station in the western Arctic Ocean

Trap station	Latitude	Longitude	Water depth (m)	Mooring depth (m)	Standard sampling interval* (days)	Sampled interval
NAP10t	75°00' N	162°00'W	1975	184 (upper), 1300 (lower)	10-15	4 October 2010–28 September 2011
NAP11t	75°00' N	162°00'W	1975	260 (upper), 1360 (lower)	10-15	4 October 2011–18 September 2012

* Details of the exact durations for each sample are shown in tables S3 and S4.

Table 3. List of 51 radiolarian taxa encountered in the plankton tow and sediment trap samples

	Taxa	References
Phylum	Rhizaria, Cavalier-Smith (2002)	
Class	Radiolaria, Müller (1858)	
Sub-class	Polycystina, Ehrenberg (1838); emend. Riedel (1967)	
Order	Spumellaria, Ehrenberg (1875)	
Family	Actinommidae, Haeckel (1862); emend. Riedel (1967)	
	Actinomma boreale, Cleve (1899)	Cortese and Bjørklund (1998), Plate 1, Figs. 1–18
	Actinomma leptodermum leptodermum, Jørgensen (1900)	Cortese and Bjørklund (1998), Plate 2, Figs. 1–14
	Actinomma morphogroup A	
	*Actinomma leptodermum,*Jørgensen (1900); *longispinum,* Cortese and Bjørklund (1998)	Cortese and Bjørklund (1998), Plate 2, Figs. 15–22
	Actinomma leptodermum longispinum juvenile	
	Actinommidae spp. juvenile forms	
	Actinomma turidae, Kruglikova and Bjørklund (2009)	Kruglikova et al. (2009), Plate 5, Figs. 1–35, Plate 6, Figs. 1–28
	Actinomma morphogroup B	
	Actinomma morphogroup B juvenile	
	**Drymyomma elegans,* Jørgensen (1900)	Dolven et al. (2014), Plate 1, Figs. 5-7
	**Actinomma friedrichdreyeri,* Burridge, Bjørklund and Kruglikova (2013)	Burridge et al. (2013), Plate 6, Figs. 7-15, Plate 7, Figs. 3-15
	Arachnosphaera dichotoma, Jørgensen (1900)	Dolven et al. (2014), Plate 1, Figs. 1-4
Family	Litheliidae, Haeckel (1862)	
	* *Streblacantha circumtexta*? Jørgensen (1905)	
Family	Spongodiscidae, Haeckel (1862)	
	Spongotrochus glacialis, Popofsky (1908)	Bjørklund et al. (1998), Plate I, Fig. 3
	Stylodictya sp.	
Order	Entactinaria, Kozur and Mostler (1982)	
	Cleveiplegma boreale, Cleve (1899)	Dumitrica (2013), Plate 1, Figs. 1-9
	Joergensenium sp. A	
	Joergensenium sp. B	
Order	Nassellaria, Ehrenberg (1875)	
Family	Sethophormididae, Haeckel (1881); emend. Petrushevskaya (1971)	
	Enneaphormis rotula, Haeckel (1881)	Petrushevskaya (1971), Fig. 31, I-III
	Enneaphormis enneastrum, Haeckel (1887)	Petrushevskaya (1971), Fig. 32, IV, V
	Protoscenium simplex, Cleve (1899)	Bjørklund et al. (2014), Plate 9, Figs. 15-17
Family	Plagiacanthidae, Hertwig (1879); emend. Petrushevskaya (1971)	
	**Arachnocorys umbellifera,* Haeckel (1862)	Welling (1996), Plate 14, Figs. 24-27
	Ceratocyrtis histricosus, Jørgensen (1905)	Petrushevskaya (1971), Fig. 52, II–IV
	Ceratocyrtis galeus, Cleve (1899)	Bjørklund et al. (2014), Plate 8, Figs. 1 and 2
	**Cladoscenium tricolpium,* Haeckel (1887)	Bjørklund (1976), Plate 7, Figs. 5-8
	Cladoscenium tricolpium?	
	*Lophophaena clevei,*Petrushevskaya (1971)	Petrushevskaya (1971), Fig. 57, I
	*Phormacantha hystrix,*Jørgensen (1900)	Dolven et al. (2014), Plate 6, Figs. 20-24
	**Peridium longispinum*?, Jørgensen (1900)	Bjørklund et al. (1998), Plate II, Figs. 26 and 27
	*Plectacantha oikiskos,*Jørgensen (1905)	Dolven et al. (2014), Plate 7, Figs. 7-9
	*Pseudodictyophimus clevei,*Jørgensen (1900)	Bjørklund et al. (2014), Plate 9, Figs. 5-7
	*Pseudodictyophimus gracilipes gracilipes,*Bailey (1856)	Bjørklund et al. (1998), Plate II, Figs. 7 and 8
	Pseudodictyophimus spp. juvenile forms	
	*Pseudiodictyophimus gracilipes,*Bailey (1856); *bicornis,*Ehrenberg (1862)	Bjørklund and Kruglikova (2003), Plate V, Figs. 16-19
	*Pseudodictyophimus gracilipes,*Bailey (1856); *multispinus,* Bernstein (1934)	Bjørklund and Kruglikova (2003), Plate V, Figs. 11-13
	*Pseudodictyophimus plathycephalus,*Haeckel (1887)	Bjørklund and Kruglikova (2003), Plate V, Figs. 1-5
	Tetraplecta pinigera, Haeckel (1887)	Takahashi (1991), Plate. 24, Figs. 1-5
	Tripodiscium (*Tholospyris*) *gephyristes,*Hülsemann (1963)	Bjørklund et al. (1998), Plate II, Figs. 20 and 21
	Plagiacanthidae gen. et sp. indet.	
Family	Eucyrtidiidae, Ehrenberg (1847); emend. Petrushevskaya (1971)	
	*Artostrobus annulatus,*Bailey (1856)	Bjørklund et al. (2014), Plate 9, Figs. 1-4
	*Artostrobus joergenseni,*Petrushevskaya (1967)	Petrushevskaya (1971), Fig. 92, VIII–IX
	**Cornutella stylophaena,*Ehrenberg (1854)	Petrushevskaya (1967), Fig. 59, I–III
	**Cornutella longiseta,*Ehreneberg (1854)	Petrushevskaya (1967), Fig. 62, I–II, Fig. 58, VIII
	*Cycladophora davisiana,*Ehrenberg (1862)	Bjørklund et al. (1998), Plate II, Figs. 1 and 6
	*Lithocampe platycephala,*Ehrenberg (1873)	Bjørklund et al. (1998), Plate II, Figs. 23–25
	*Lithocampe aff. furcaspiculata,*Popofsky (1908)	Petrushevskaya (1967), Fig. 74, I–IV
	*Sethoconus tabulatus,*Ehrenberg (1873)	Bjørklund et al. (2014), Plate 9, Figs. 10 and 11
Family	Cannobotryidae, Haeckel (1881); emend. Riedel (1967)	
	*Amphimelissa setosa,*Cleve (1899)	Bjørklund et al. (1998), Plate II, Figs. 30–33
	Amphimelissa setosa juvenile	
Class	Cercozoa, Cavalier-Smith (1998); emend. Adl et al. (2005)	
Order	Phaeodaria, Haeckel (1879)	
	*Lirella melo,*Cleve (1899)	Bjørklund et al. (2014), Plate 11, Figs. 5 and 6
	*Protocystis harstoni,*Murray (1885)	Takahashi and Honjo (1981), Plate 11, Fig. 11

All taxa are found in the trap, and * refers to taxa found in trap only.

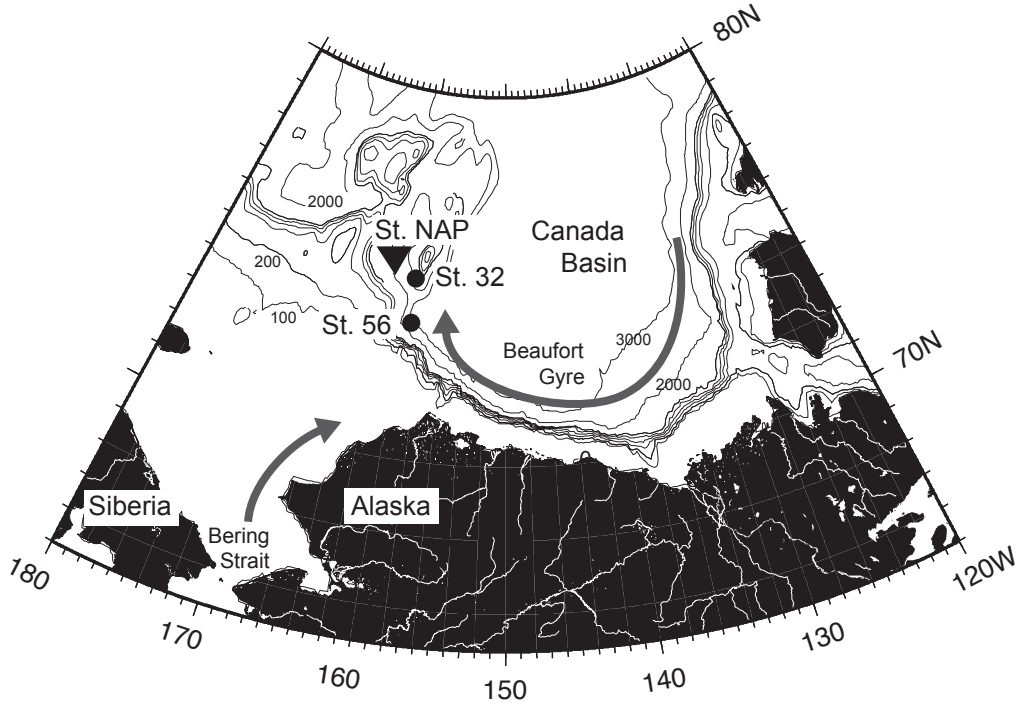
80N
70N
120W
180
170
160
150
140
130
2000
200
100
St. NAP
St. 32
St. 56
Canada
Basin
Beaufort
Gyre
3000
2000
Siberia
Alaska
Bering
Strait

Fig. 1

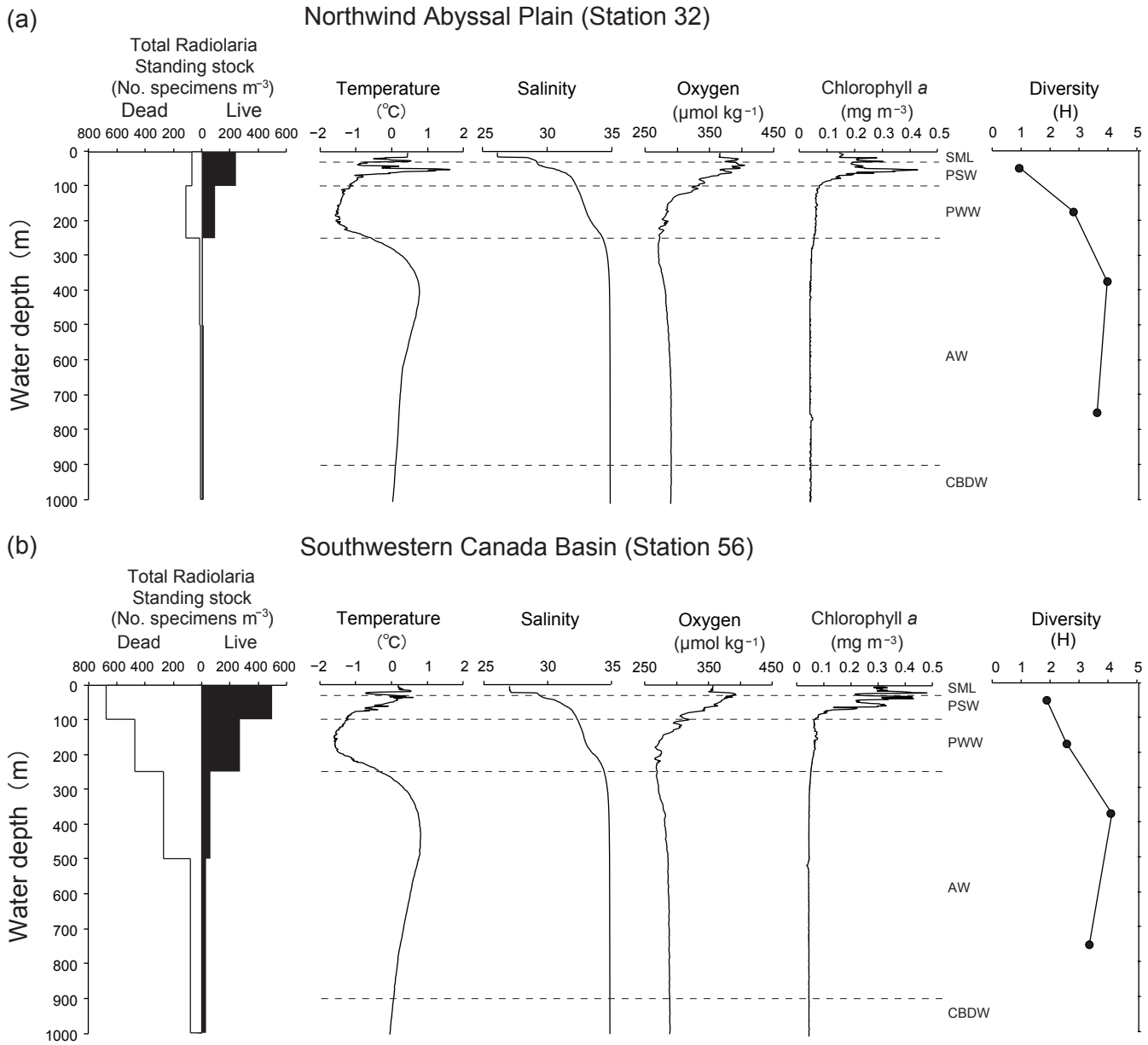
(a)
Northwind Abyssal Plain (Station 32)
Total Radiolaria
Standing stock
(No. specimens m⁻³)
Dead
Live
Temperature
(℃)
Salinity
Oxygen
(μmol kg⁻¹)
Chlorophyll a
(mg m⁻³)
Diversity
(H)
Water depth (m)
SML
PSW
PWW
AW
CBDW
(b)
Southwestern Canada Basin (Station 56)

Fig. 2

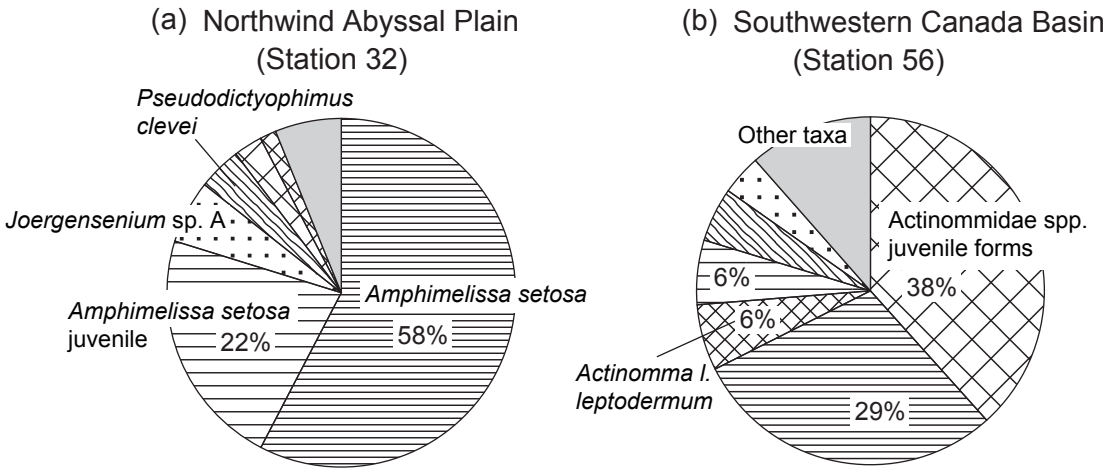
(a) Northwind Abyssal Plain
(Station 32)
Pseudodictyophimus clevei
Joergensenium sp. A
Amphimelissa setosa
Amphimelissa setosa juvenile
22%
58%
(b) Southwestern Canada Basin
(Station 56)
Other taxa
Actinommidae spp. juvenile forms
6%
38%
6%
Actinomma l. leptodermum
29%

Fig. 3

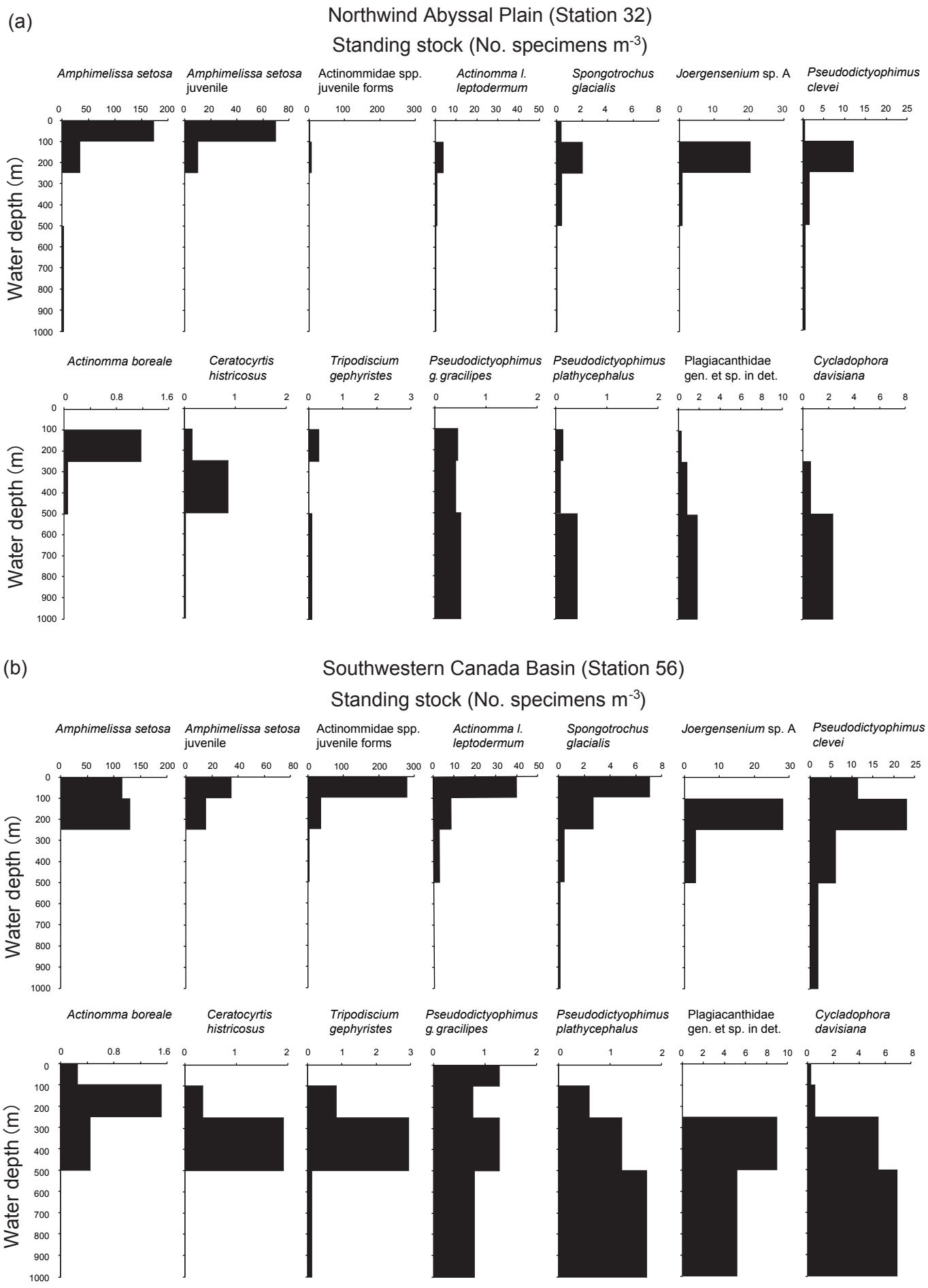
(a)
Northwind Abyssal Plain (Station 32)
Standing stock (No. specimens m-3)
Amphimelissa setosa
Amphimelissa setosa juvenile
Actinommidae spp. juvenile forms
Actinomma l. leptodermum
Spongotrochus glacialis
Joergensenium sp. A
Pseudodictyophimus clevei
Actinomma boreale
Ceratocyrtis histricosus
Tripodiscium gephyristes
Pseudodictyophimus g. gracilipes
Pseudodictyophimus plathycephalus
Plagiacanthidae gen. et sp. in det.
Cycladophora davisiana
Water depth (m)
(b)
Southwestern Canada Basin (Station 56)
Standing stock (No. specimens m-3)
Amphimelissa setosa
Amphimelissa setosa juvenile
Actinommidae spp. juvenile forms
Actinomma l. leptodermum
Spongotrochus glacialis
Joergensenium sp. A
Pseudodictyophimus clevei
Actinomma boreale
Ceratocyrtis histricosus
Tripodiscium gephyristes
Pseudodictyophimus g. gracilipes
Pseudodictyophimus plathycephalus
Plagiacanthidae gen. et sp. in det.
Cycladophora davisiana
Water depth (m)

Fig. 4

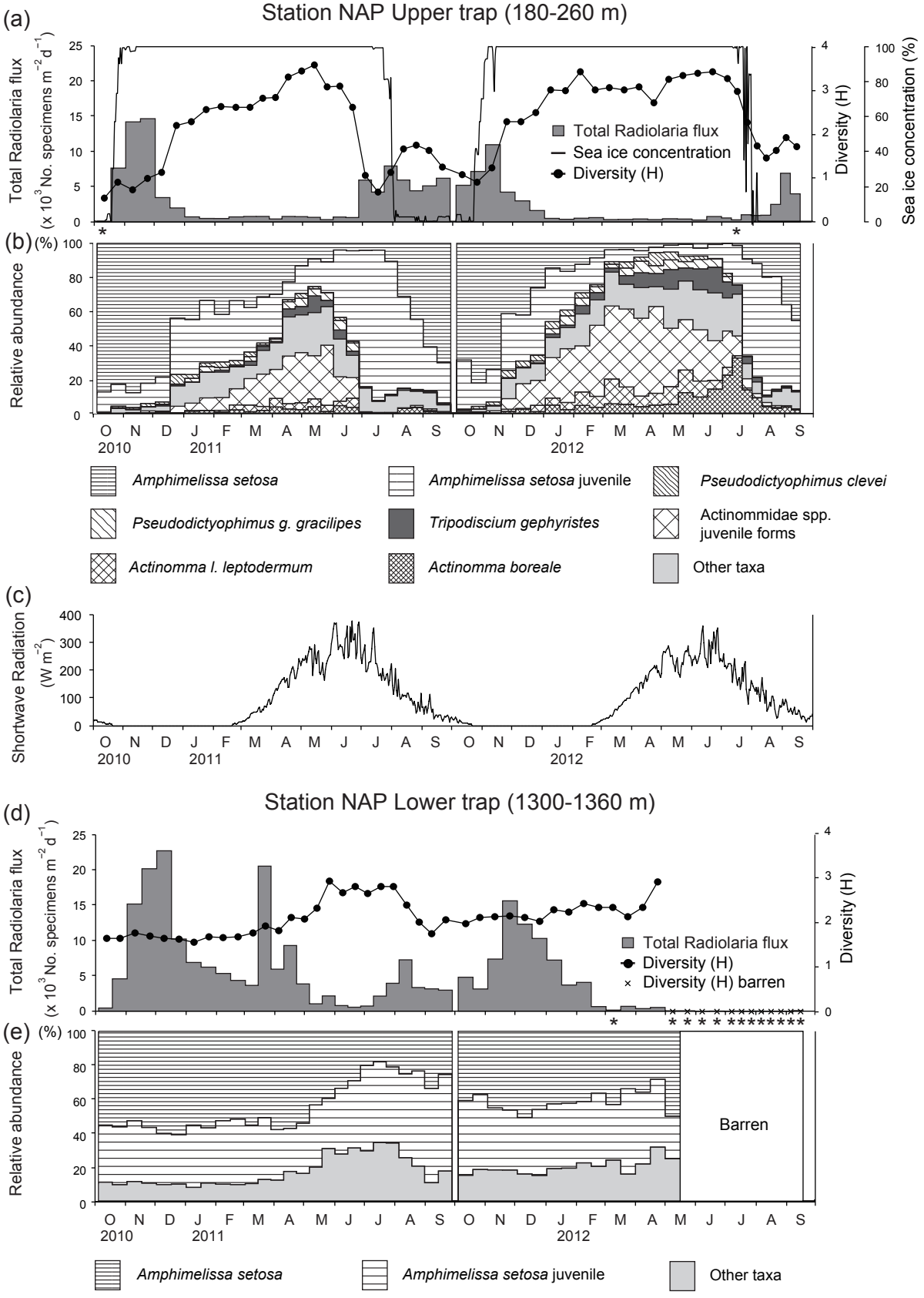
(a)
Station NAP Upper trap (180-260 m)
Total Radiolaria flux (x 10^3 No. specimens m^-2 d^-1)
Diversity (H)
Sea ice concentration (%)
Total Radiolaria flux
Sea ice concentration
Diversity (H)
(b)
(%)
Relative abundance
O N D J F M A M J J A S O N D J F M A M J J A S
2010
2011
2012
Amphimelissa setosa
Amphimelissa setosa juvenile
Pseudodictyophimus clevei
Pseudodictyophimus g. gracilipes
Tripodiscium gephyristes
Actinommidae spp. juvenile forms
Actinomma l. leptodermum
Actinomma boreale
Other taxa
(c)
Shortwave Radiation (W m^-2)
(d)
Station NAP Lower trap (1300-1360 m)
Total Radiolaria flux (x 10^3 No. specimens m^-2 d^-1)
Diversity (H)
Total Radiolaria flux
Diversity (H)
Diversity (H) barren
(e)
(%)
Relative abundance
Barren
Amphimelissa setosa
Amphimelissa setosa juvenile
Other taxa

Fig. 5

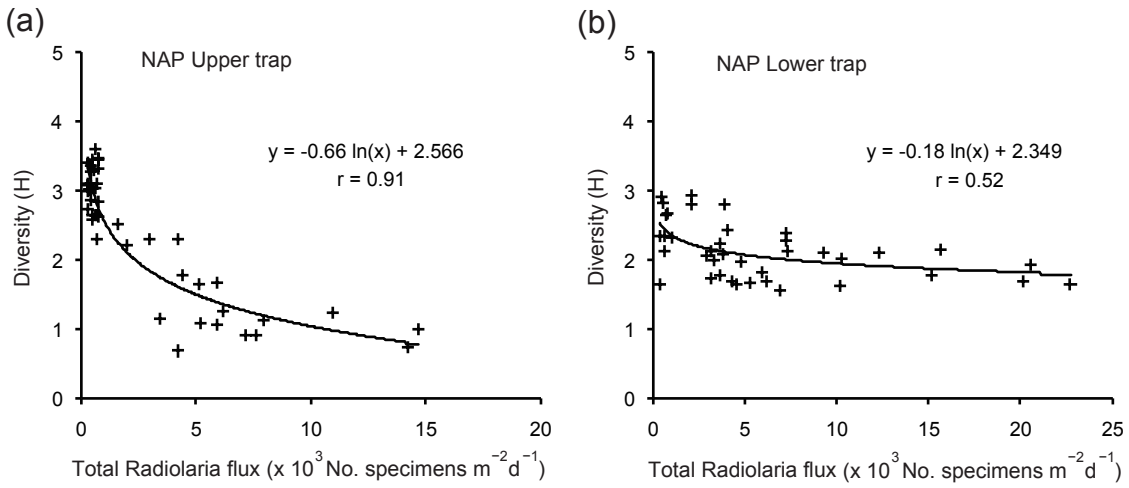
(a)
NAP Upper trap
y = -0.66 ln(x) + 2.566
r = 0.91
Diversity (H)
Total Radiolaria flux (x 10^3 No. specimens m^-2 d^-1)
(b)
NAP Lower trap
y = -0.18 ln(x) + 2.349
r = 0.52
Diversity (H)
Total Radiolaria flux (x 10^3 No. specimens m^-2 d^-1)

Fig. 6

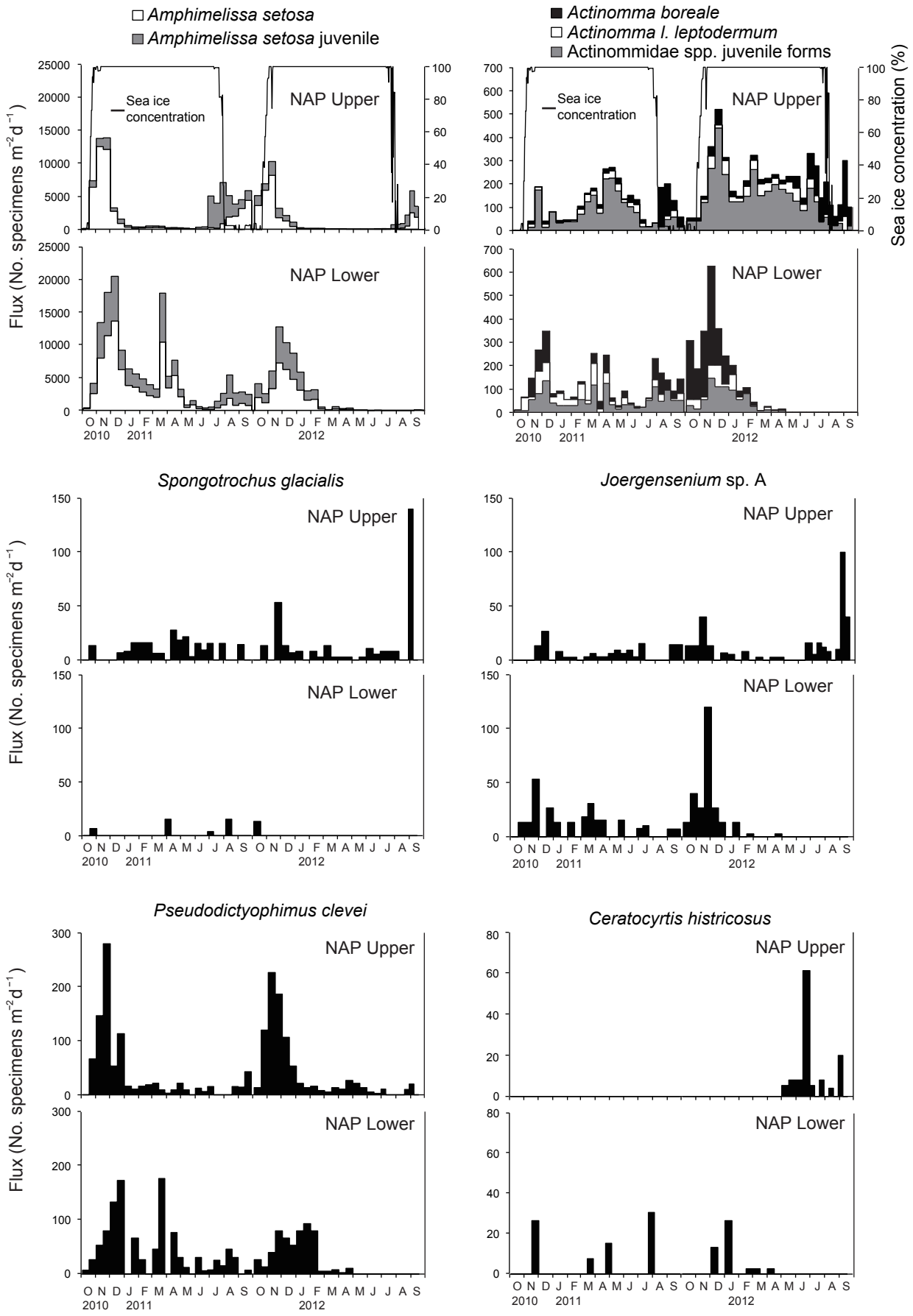
□ Amphimelissa setosa
■ Amphimelissa setosa juvenile
■ Actinomma boreale
□ Actinomma l. leptodermum
■ Actinommidae spp. juvenile forms
Sea ice concentration
NAP Upper
NAP Lower
Flux (No. specimens m-2 d-1)
Sea ice concentration (%)
Spongotrochus glacialis
Joergensenium sp. A
Pseudodictyophimus clevei
Ceratocyrtis histricosus
O N D J F M A M J J A S O N D J F M A M J J A S
2010 2011 2012

Fig. 7

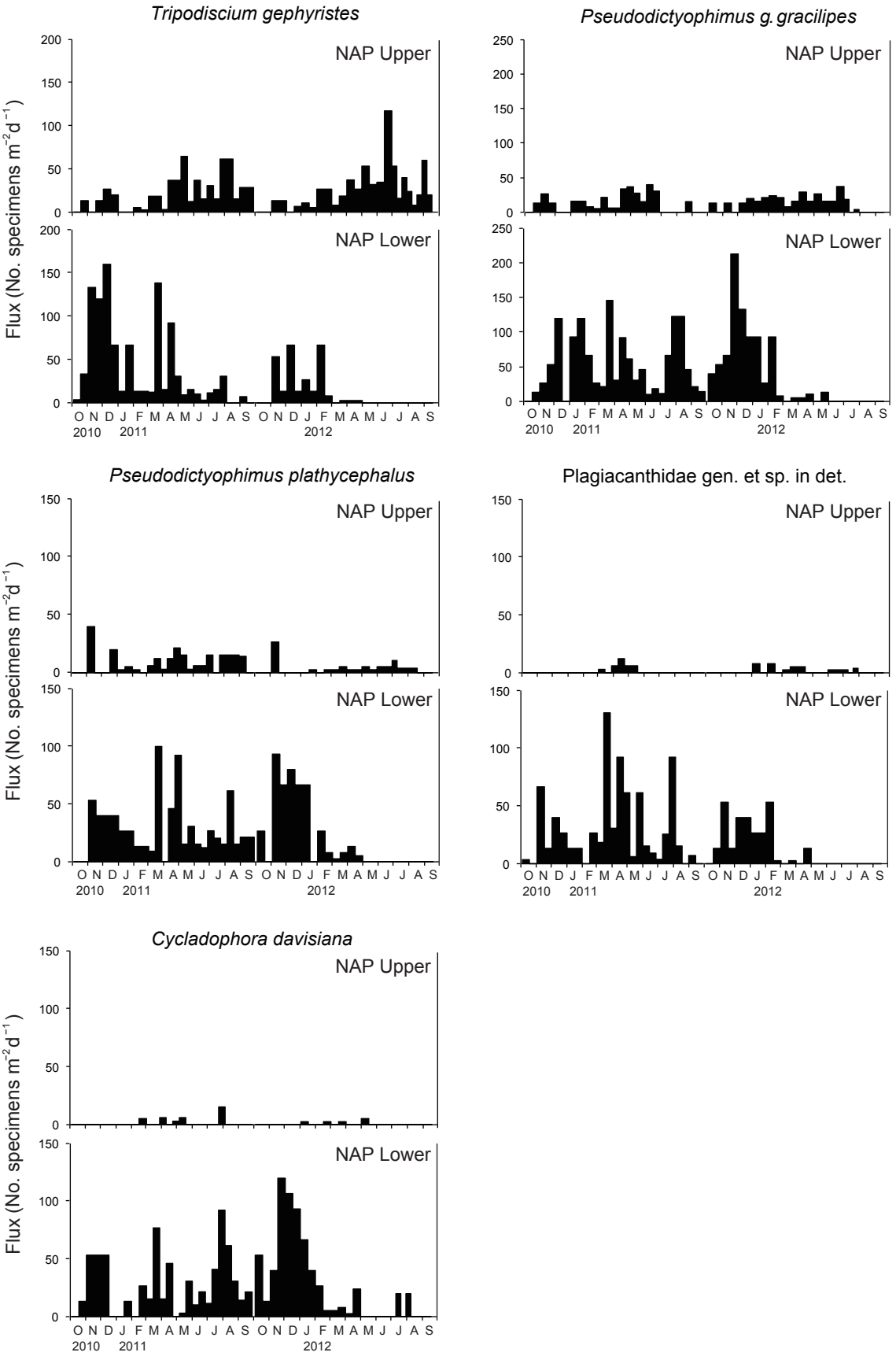

Fig. 7 (continued)

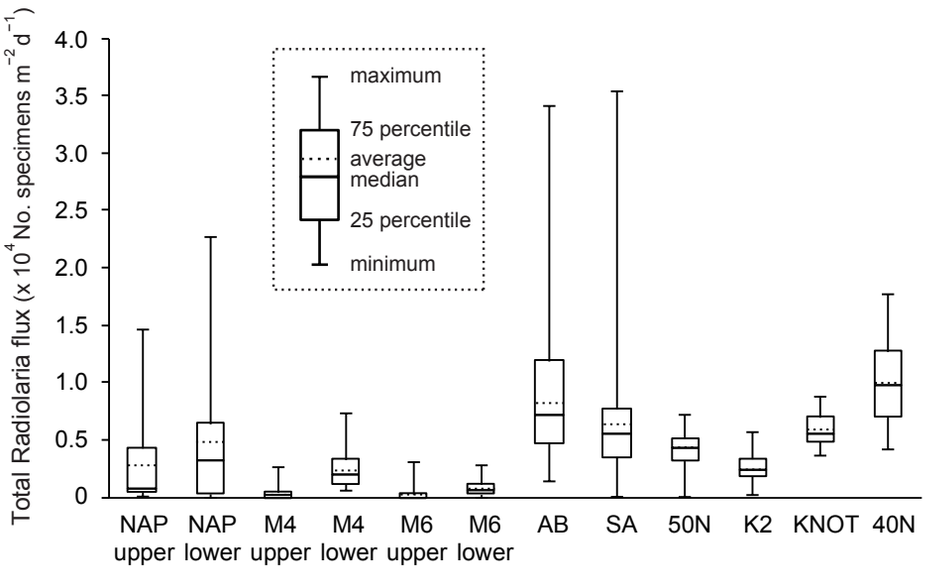
Total Radiolaria flux (x 10^4 No. specimens m^-2 d^-1)
4.0
3.5
3.0
2.5
2.0
1.5
1.0
0.5
0
maximum
75 percentile
average
median
25 percentile
minimum
NAP upper
NAP lower
M4 upper
M4 lower
M6 upper
M6 lower
AB
SA
50N
K2
KNOT
40N

Fig. 8

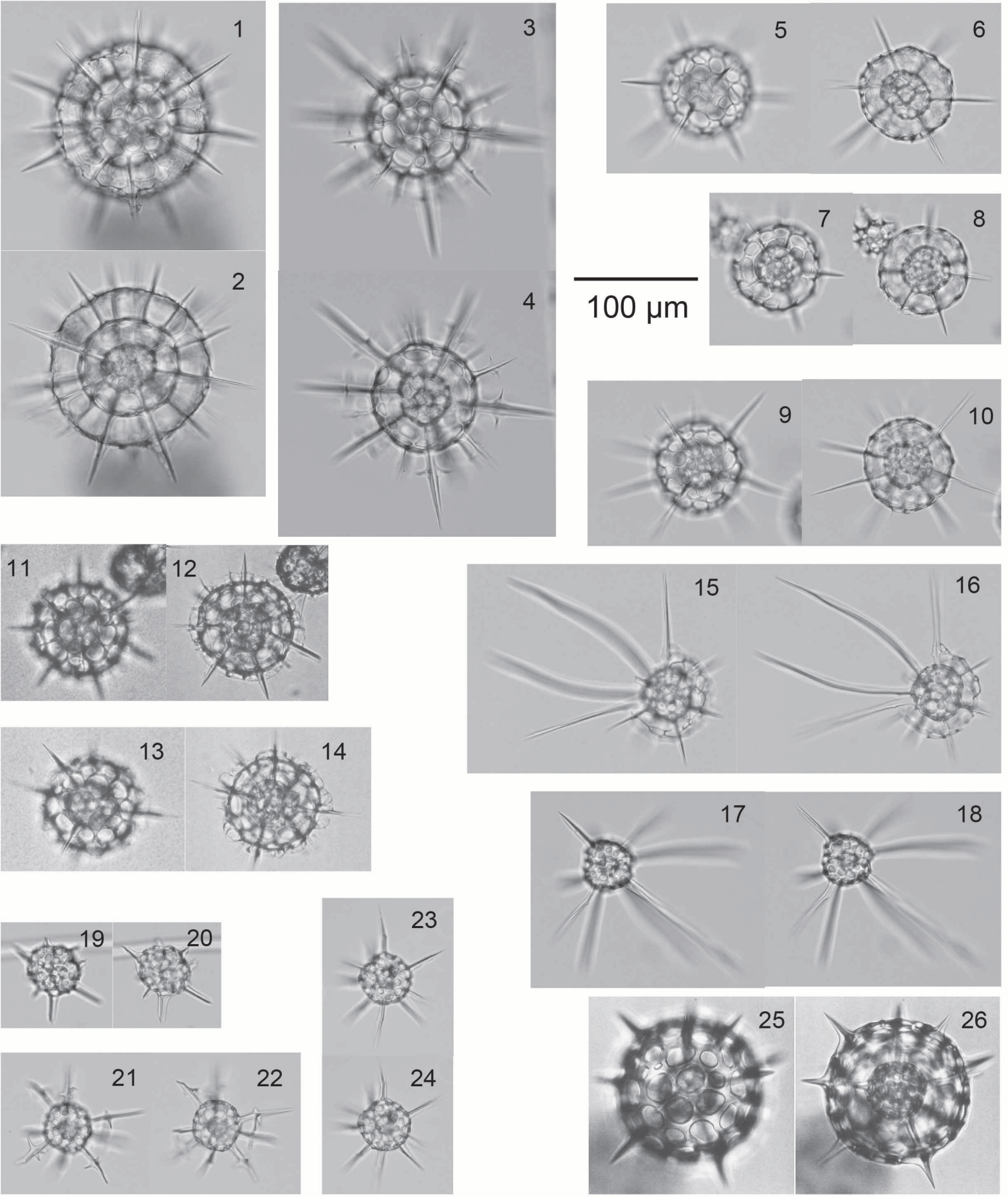

Plate 1

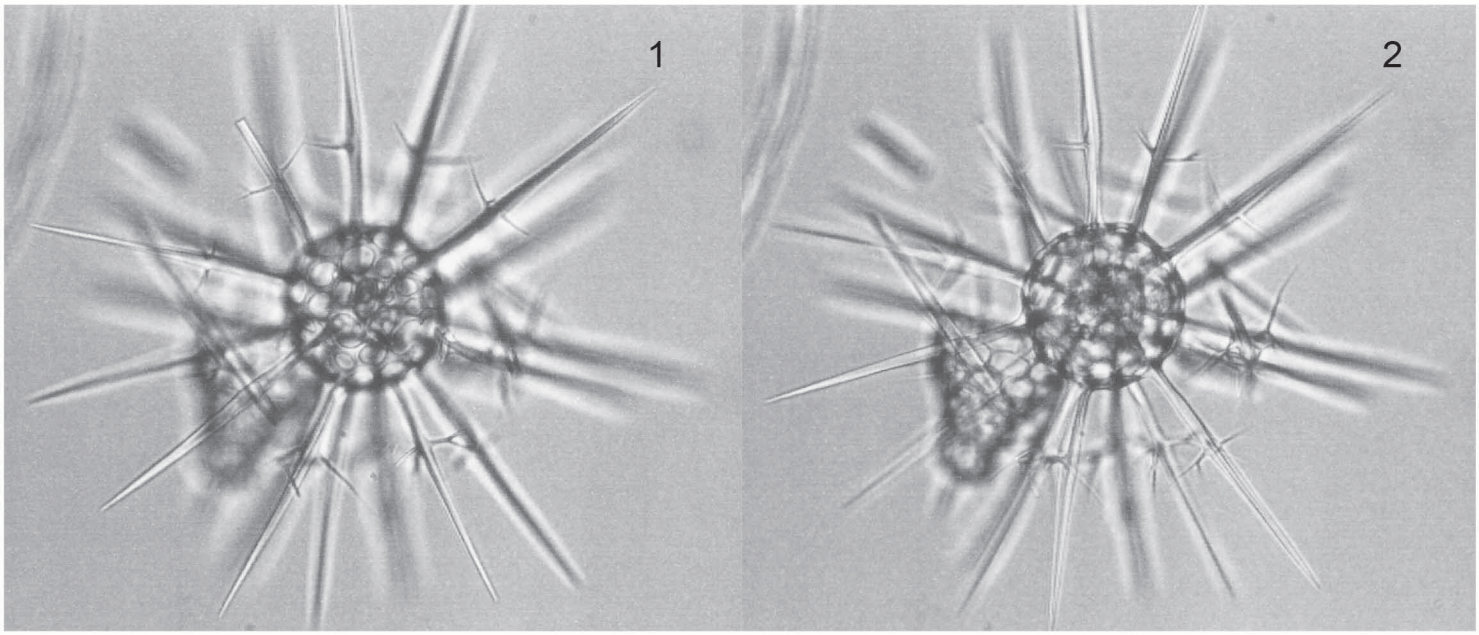

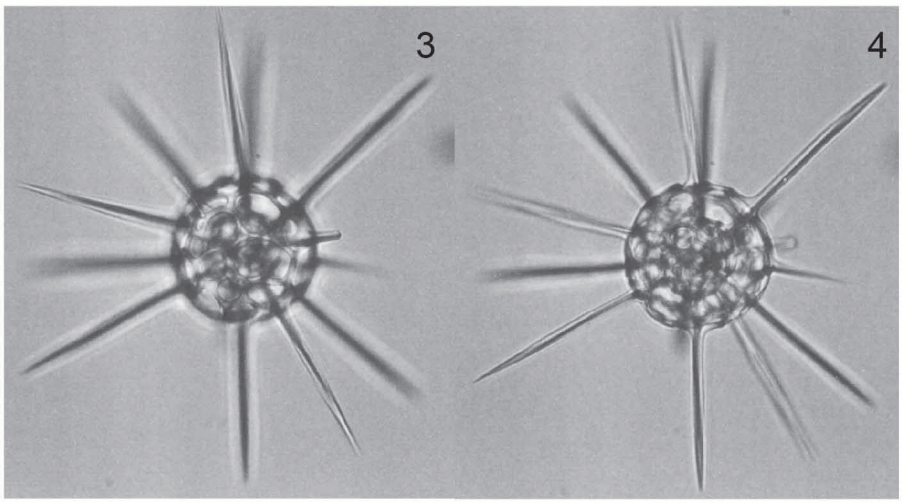

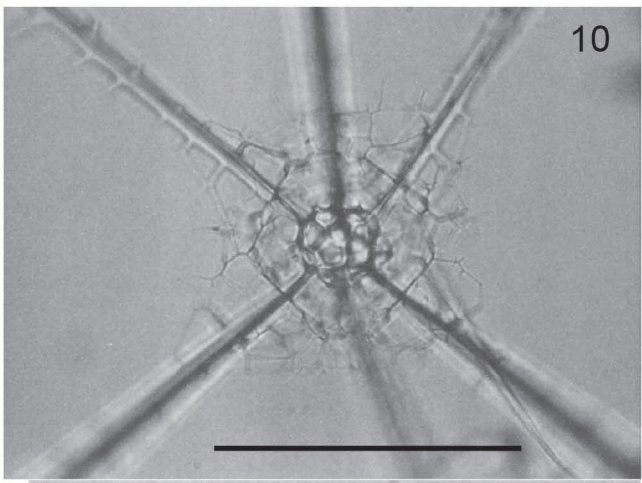

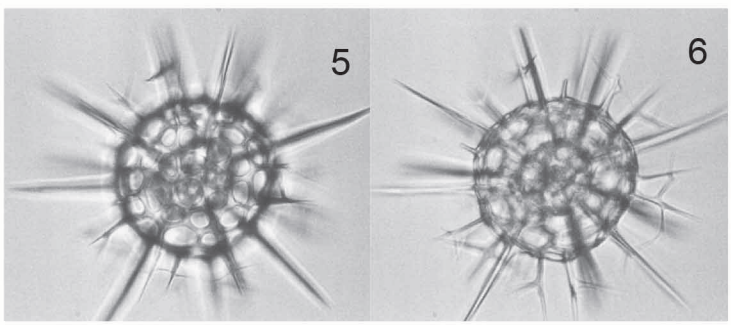

100 µm

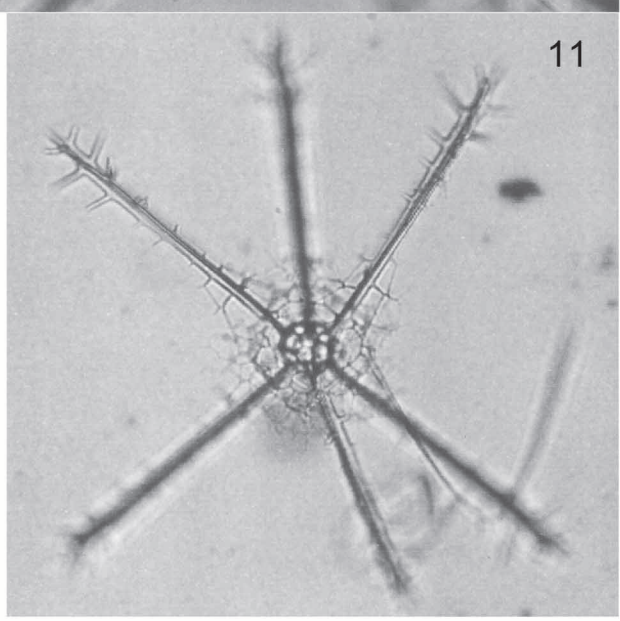

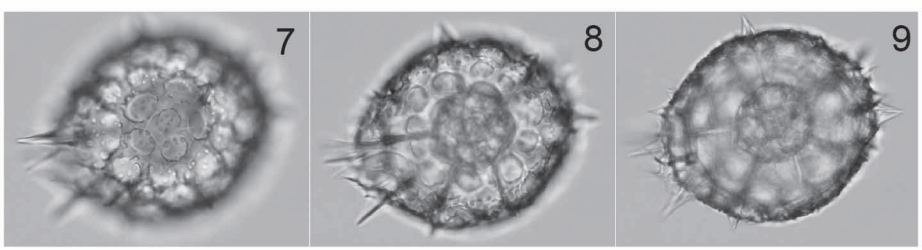

Plate 2

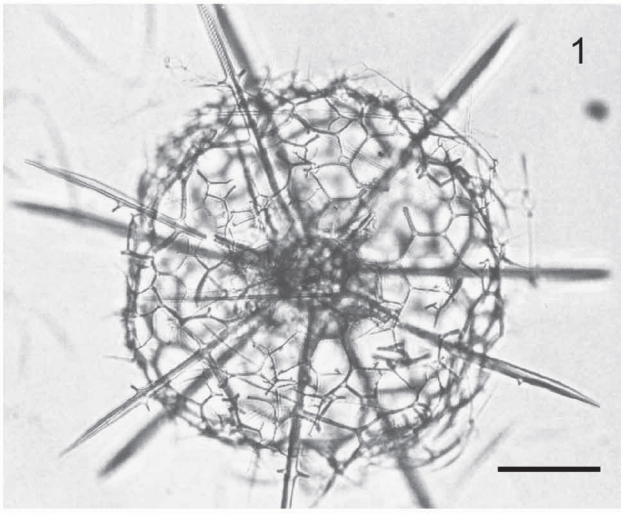

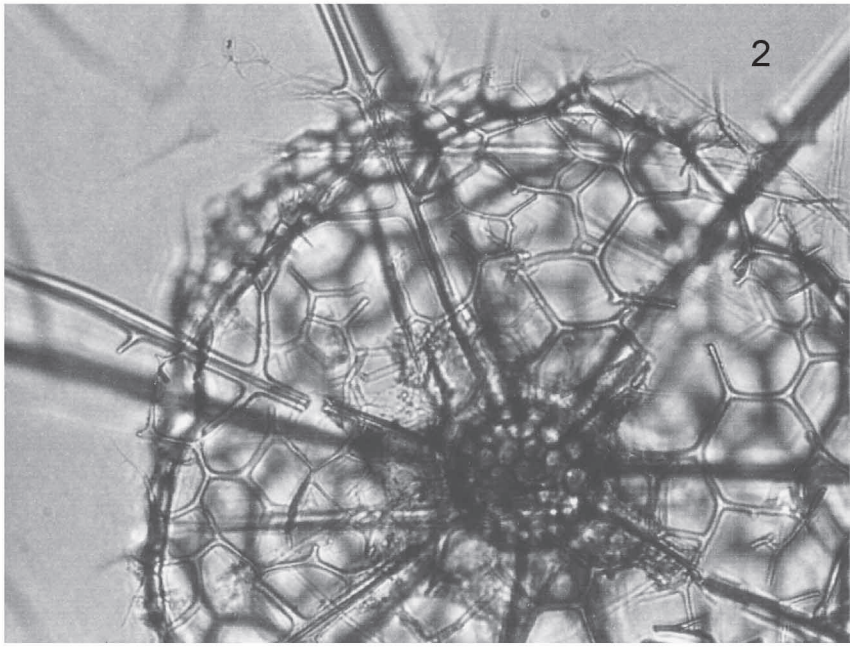

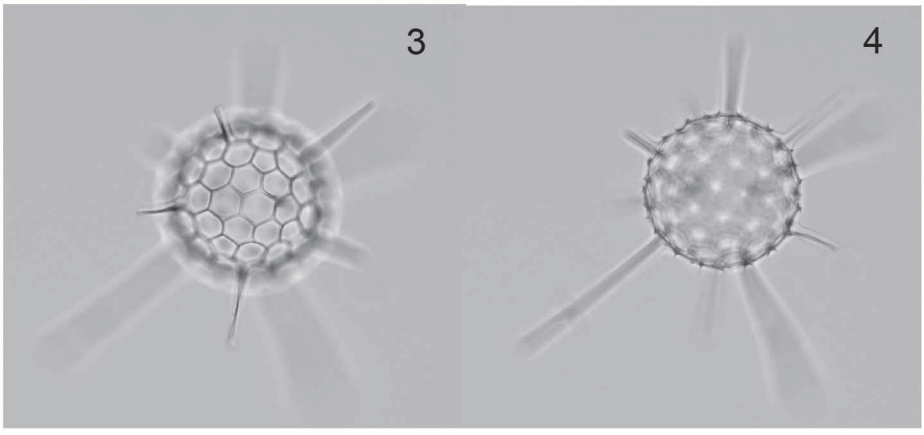

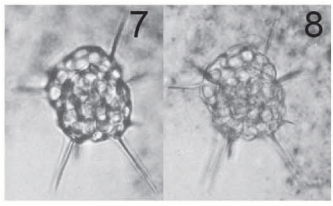

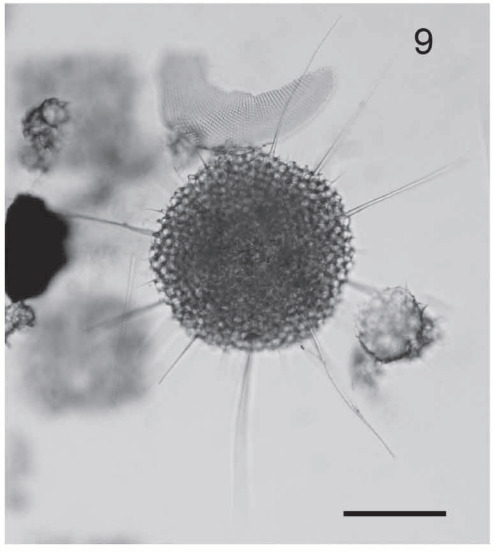

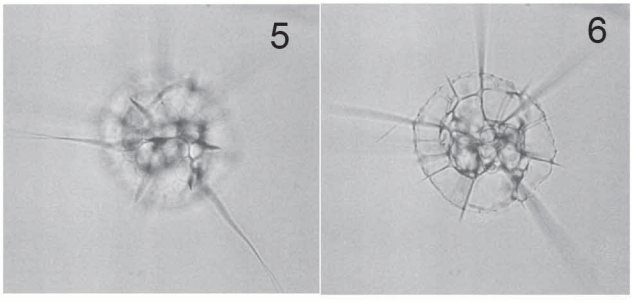

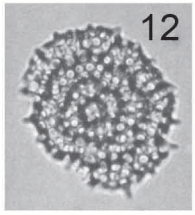

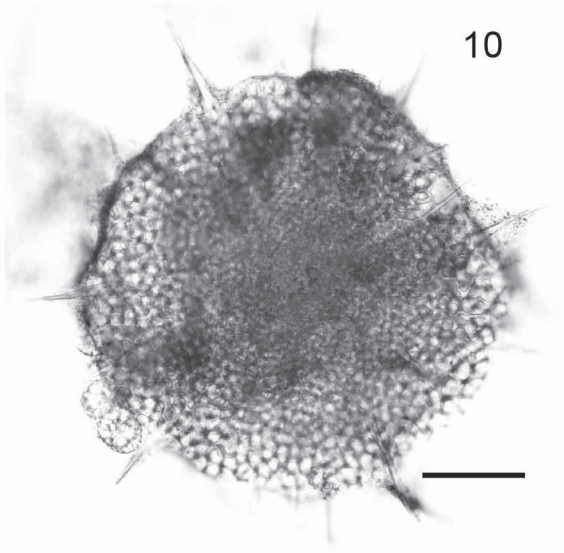

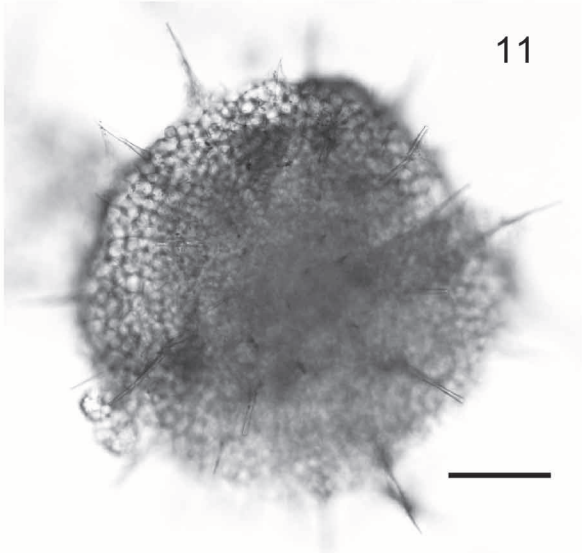

100 µm

Plate 3

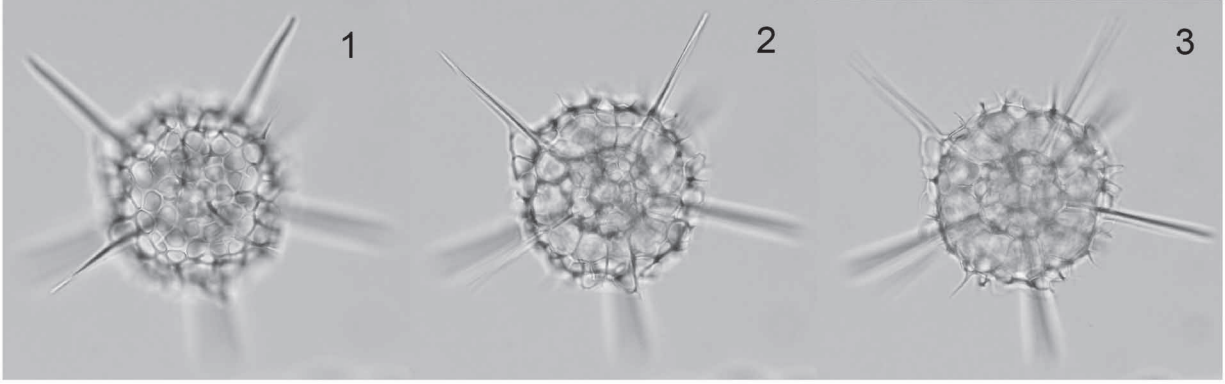

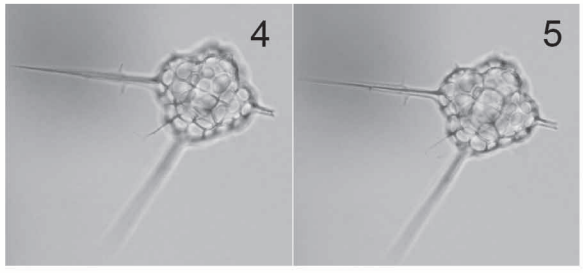

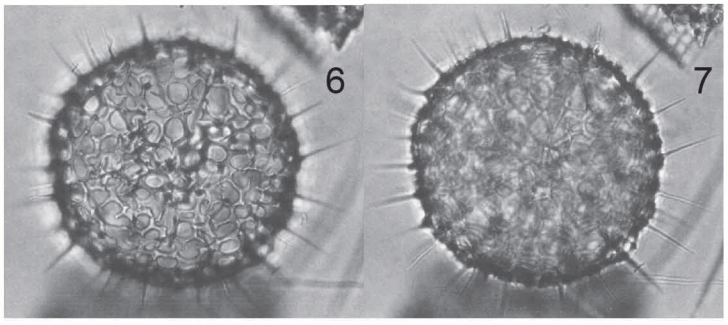

100 µm

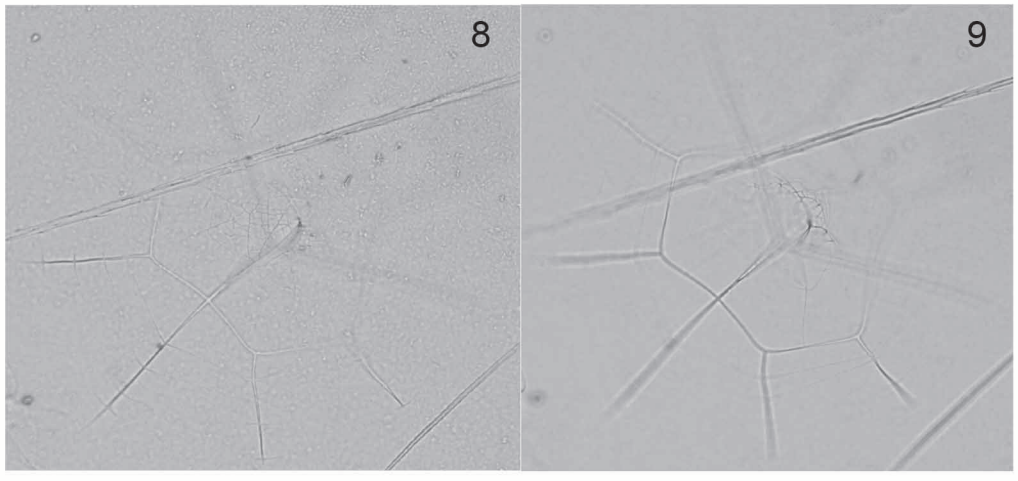

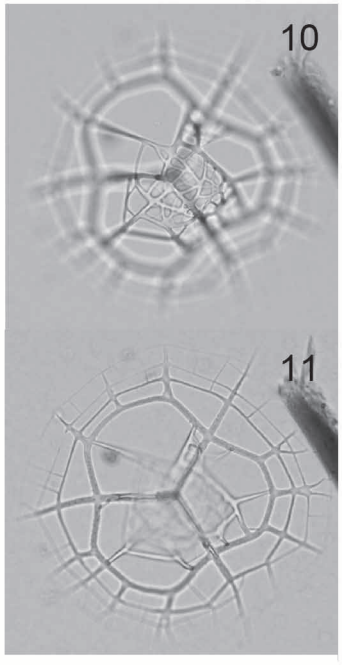

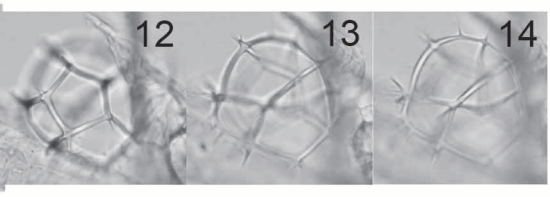

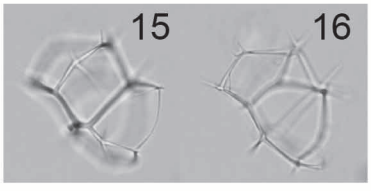

Plate 4

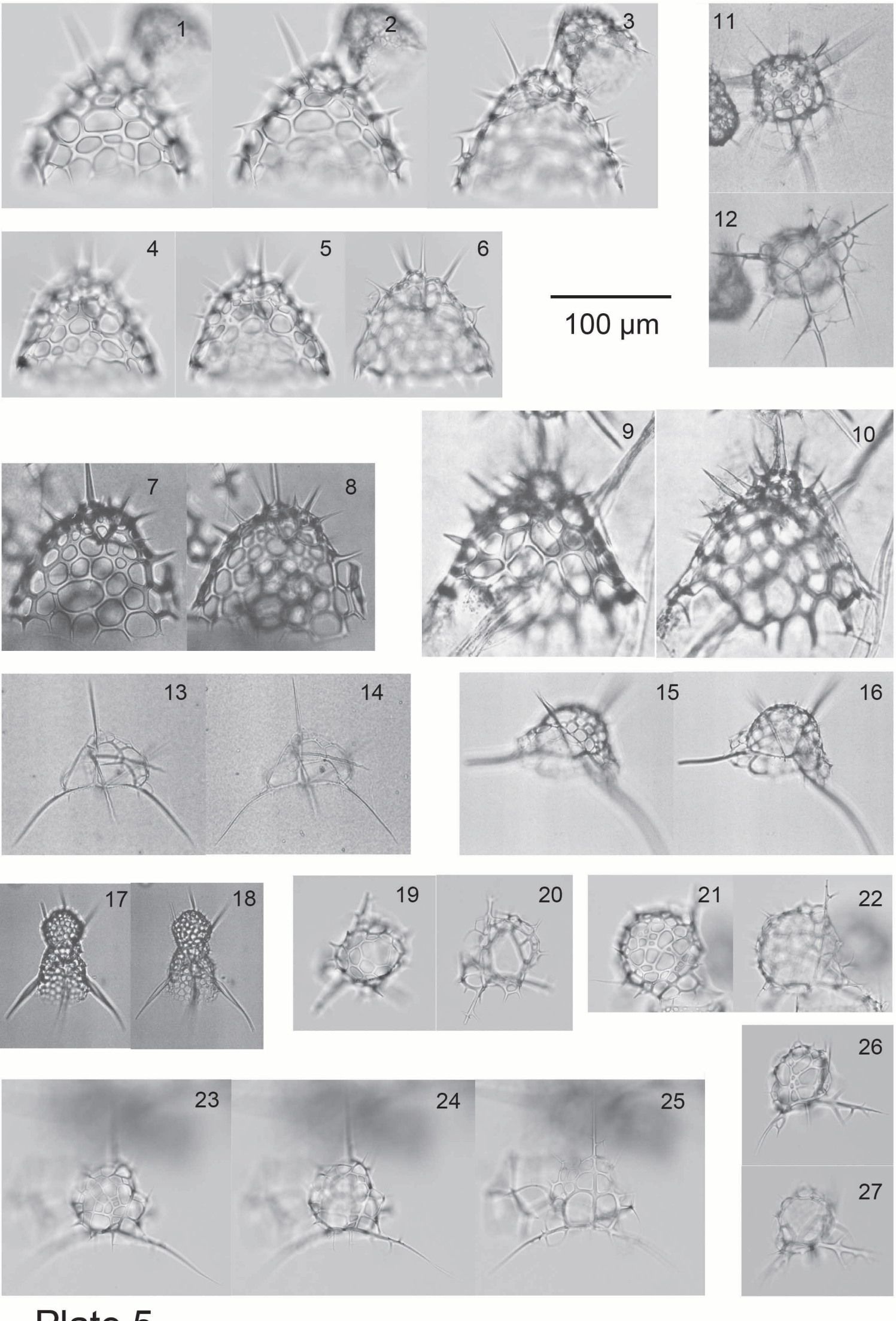
1
2
3
11
12
4
5
6
100 µm
9
10
7
8
13
14
15
16
17
18
19
20
21
22
26
23
24
25
27

Plate 5

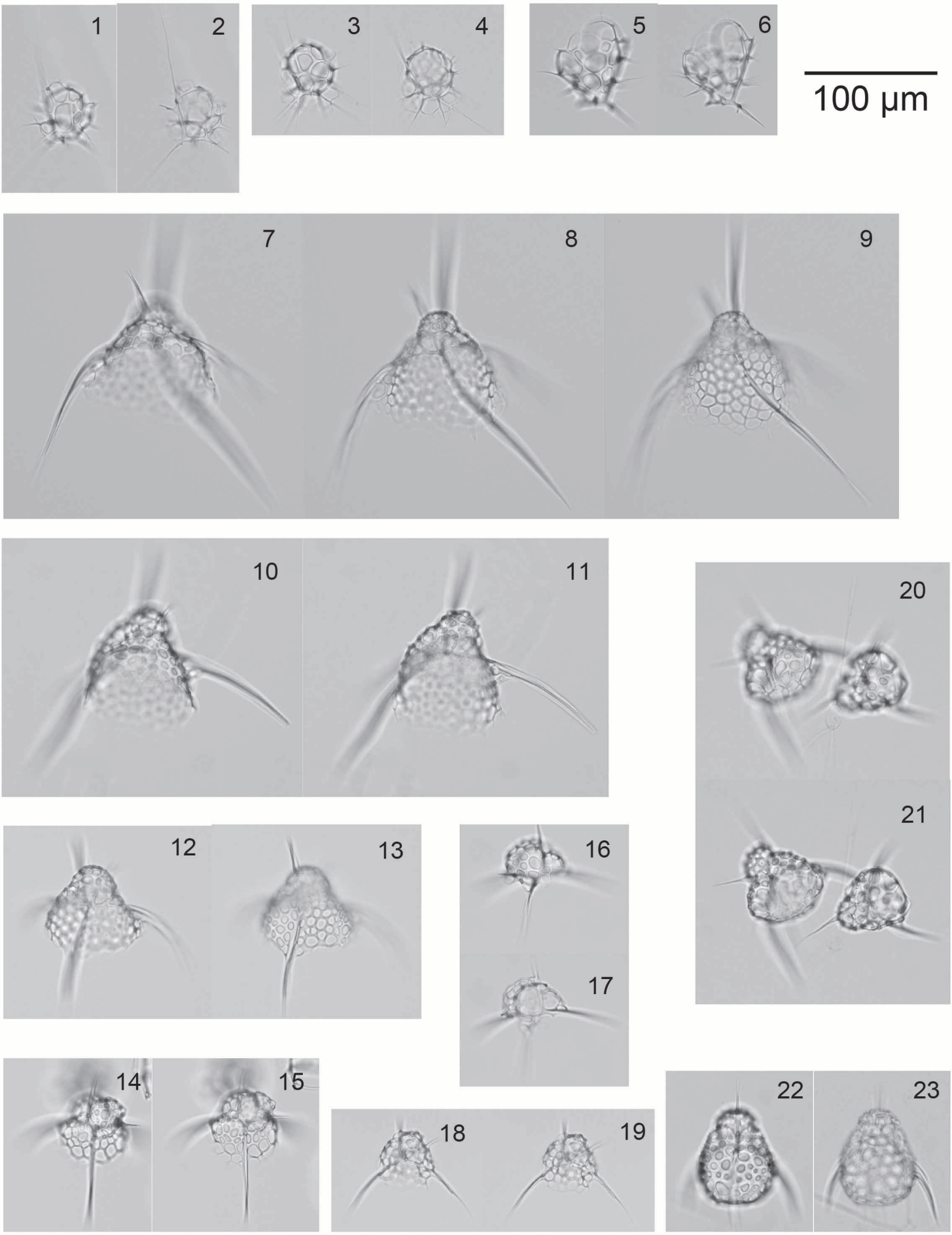

Plate 6

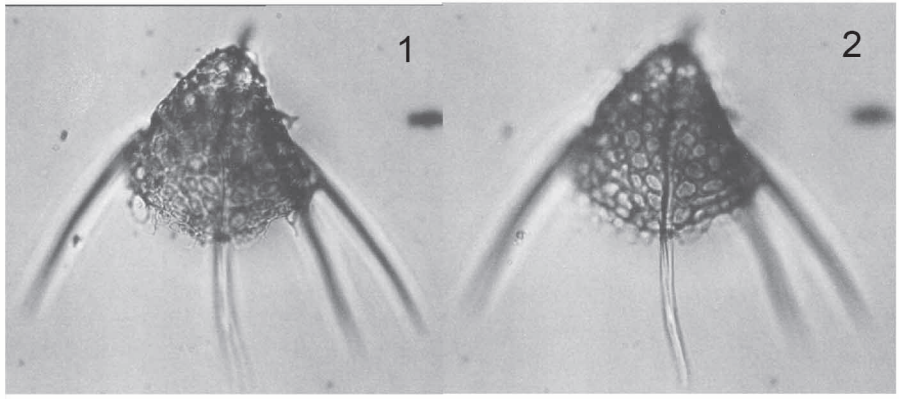

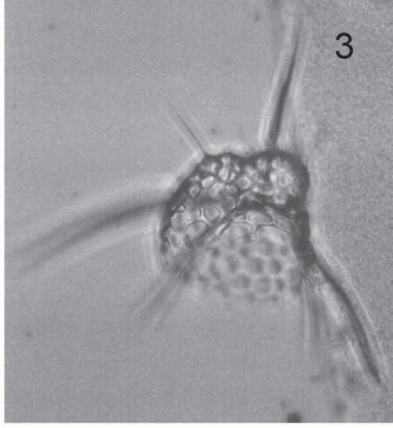

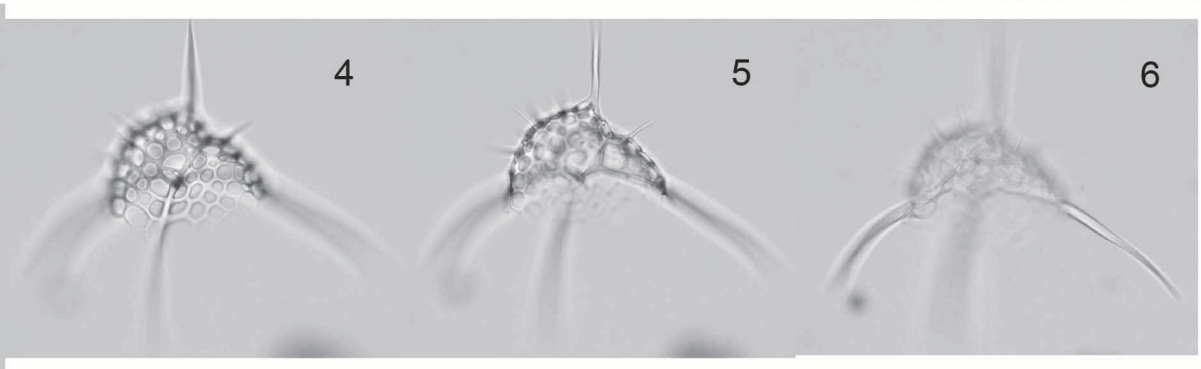

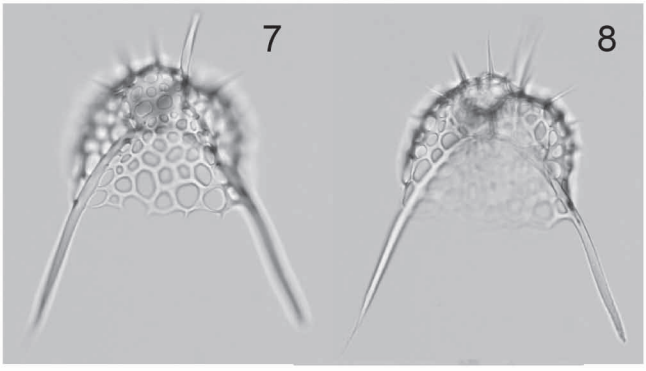

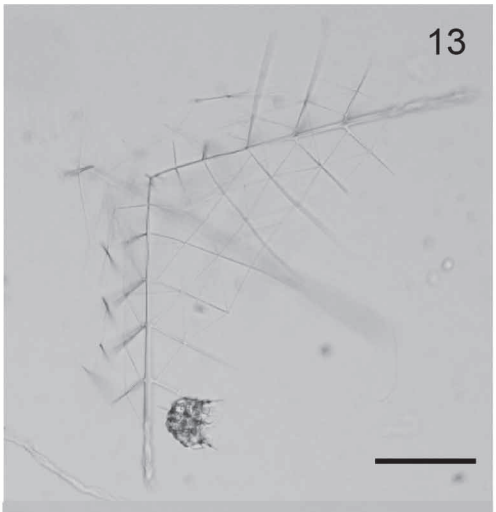

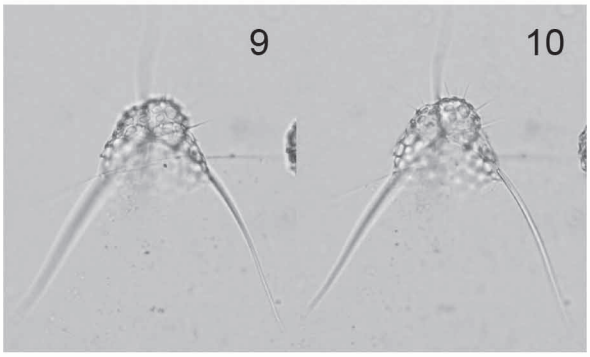

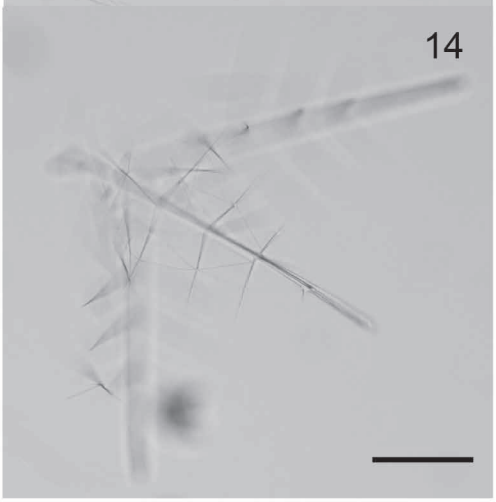

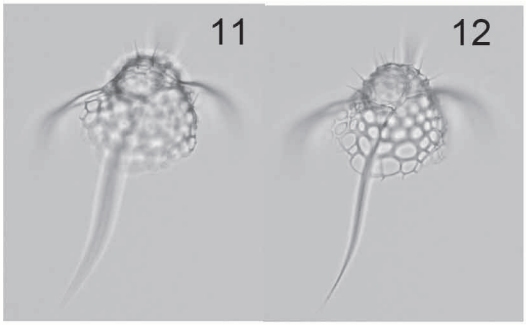

100 µm

Plate 7

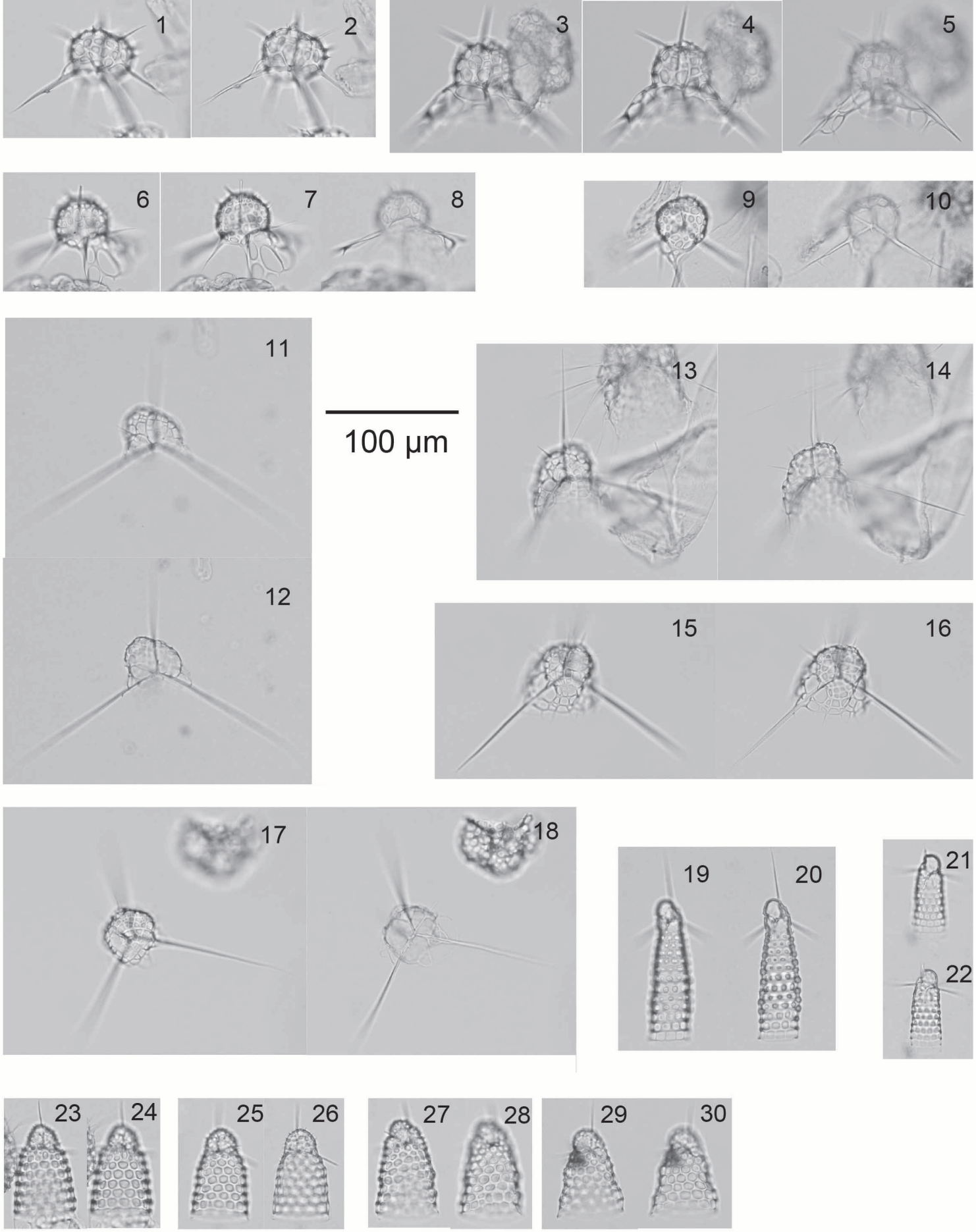
1
2
3
4
5
6
7
8
9
10
11
100 µm
13
14
12
15
16
17
18
19
20
21
22
23
24
25
26
27
28
29
30

Plate 8

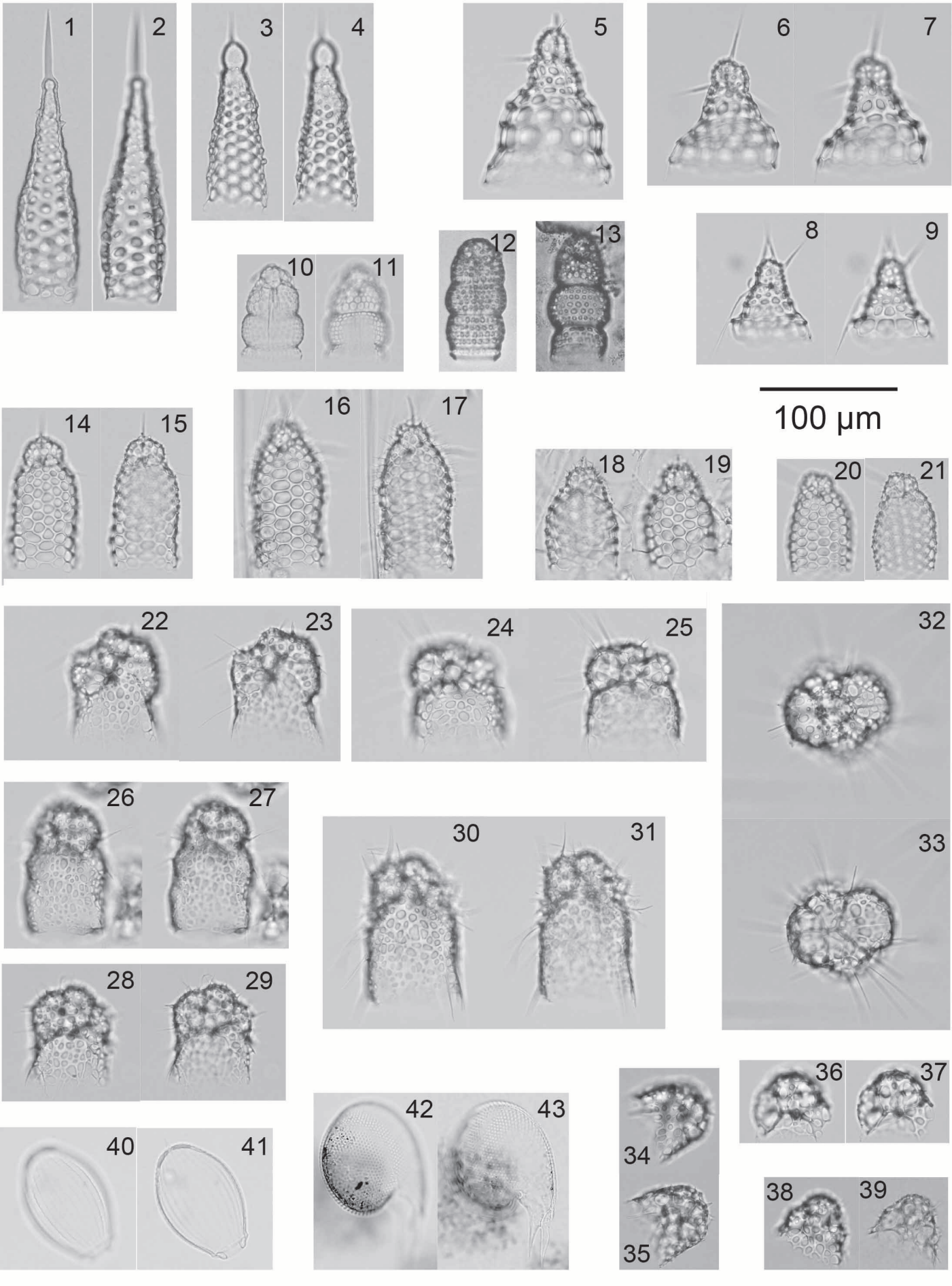
1
2
3
4
5
6
7
8
9
10
11
12
13
100 µm
14
15
16
17
18
19
20
21
22
23
24
25
32
26
27
30
31
33
28
29
42
43
34
35
36
37
38
39
40
41

Plate 9